

We can't solve problems by using the same kind of thinking we used when we created them.

Albert Einstein

4-D WORLD – UNIVERSE MODEL

OVERVIEW

Vladimir S. Netchitailo

Biolase Inc., 4 Cromwell, Irvine CA 92618, USA. v.netchitailo@sbcglobal.net

ABSTRACT

This paper provides an overview of the 4-D World – Universe Model (WUM). The World – Universe Model unifies and simplifies existing Cosmological models and results into a single coherent picture, and proceeds to compare the origin, evolution, structure, ultimate fate, and parameters of the World to the Big Bang Model.

WUM explains the experimental data accumulated in the field of Cosmology and Astroparticle Physics over the last decades: the size and age of the World; critical energy density and the gravitational parameter; temperatures of the cosmic microwave background radiation and the peak of the far-infrared radiation; observed expansion of the World and cosmological redshift; gamma-ray background and macrostructure of the World. Additionally, the Model makes predictions pertaining to masses of dark matter particles, photons, axions, and neutrinos; proposes new types of particle interactions (Super Weak and Extremely Weak) and the fundamental physical parameters of the World; explains “Pioneer Anomaly” and the rise of the solar luminosity steadily from about 70% of its current value during the last 4.6 Byr.

The Model proposes to introduce a new fundamental parameter Q in the CODATA internationally recommended values for calculating time dependent parameters of the World.

Introduction	3
1. Cosmology	5
1.1. The Beginning and Expansion	5
1.2. The World's Matter Content	5
1.3. Horizon and Flatness	5
1.4. The Creation of Matter	5
1.5. Newtonian Parameter of Gravitation	7
1.6. Time Varying Parameters of the World	7
1.7. Macroobjects of the World. Pioneer Anomaly	9
1.8. Nucleosynthesis	11
1.9. Cosmological Redshift	11
2. Comparing World - Universe Model and Big Bang Model	12
2.1. The Beginning and Expansion	12
2.2. The Size and Age of the World	12
2.3. Horizon and Flatness	13
2.4. The Creation of Matter	13
2.5. Newtonian Parameter of Gravitation	13
2.6. Nucleosynthesis	13
2.7. Microwave Background Radiation	13
2.8. Formation and Evolution of Large-Scale Structures	14
2.9. Cosmological Redshift. Dark Energy	14
2.10. Ultimate Fate of the Universe	15
3. Astroparticle Physics	15
3.1. Basic Unit of Mass	15
3.2. Low Density Plasma. Temperature of the Microwave Background Radiation	15
3.3. Mass Varying Photons. Speed of Light	16
3.4. Mass Varying Neutrinos	17
3.5. Cosmic Far-Infrared Background	18
3.6. Multi-Component Dark Matter	24
3.7. Macroobjects Cores Built up from Fermionic Dark Matter	25
3.8. Dark Matter Signatures in Gamma-Ray Spectra	28
3.9. Grand Unified Theory	36

INTRODUCTION

Today, a growing feeling of stagnation is shared by a large number of researchers. In his "The Twilight of the Scientific Age" (2013), Martin Lopez Corredoira outlines everything that is wrong with Physics today: increasingly expensive experiments that yield less and less, lack of outstanding results, lack of openness to new ideas exhibited by scientific journals and community as a whole.

In some respects, the situation today is similar to that at the end of 19th century, when the common consensus held that the body of Physics is nearly complete. Discoveries of special and general relativity, quantum mechanics and elementary particles shook that belief and led to a new renaissance in Physics that lasted for a century. The genius of Einstein, Bohr, Dirac, Heisenberg, and Schrödinger allowed them to propose fundamentally new theories with very little experimental data to back them up.

During the 20th century, their theories were validated and elaborated with newly acquired experimental results. The pendulum may, however, have swung too far: today, all results must be made fit into the existing framework. The frameworks get adjusted when necessary, particularly inconvenient results may even get discarded at times. The time may be ripe to propose new fundamental models that will be both simpler than the current state of the art, as well as open up new areas of research.

In 1870, William Clifford made the statement that matter is nothing but ripples, hills and bumps of space curved in a higher dimension and the motion of matter is nothing more than variations in that curvature. He speculated that the force of electricity and magnetism is caused by the bending of higher-dimensional space and planned to add gravity to his theory at later date.

*"This is the first time that anyone had speculated that a "force" is nothing but the bending of space itself, preceding Einstein by 50 years. Clifford's idea that electromagnetism was caused by vibrations in the fourth dimension also preceded the work of Theodor Kaluza, who would also attempt to explain electromagnetism with the higher dimension. For the first time, someone correctly isolated the true physical meaning of higher dimensions, that a theory about **space** actually gives us a unifying picture of **forces**"* (Michio Kaku, *Hyperspace*. Oxford University Press, 1994).

4-D World – Universe Model follows this idea of the fourth spatial dimension, albeit introducing the Medium of the World instead of empty space.

In 1937, Paul Dirac proposed a new basis for cosmology: the hypothesis of a variable gravitational "constant" [1]; and later added the notion of continuous creation of matter in the World [2]. World – Universe Model follows these ideas, albeit introducing a different mechanism of matter creation.

In the present work we are giving an overview of the World – Universe Model (WUM) which is unifying and simplifying existing models and results in Cosmology into a single coherent picture. The Model was developed in papers [3 – 10]. WUM is proposed as an alternative to the prevailing Bing Bang Model (BBM) of standard physical cosmology. The main difference is the source of the World's energy.

World – Universe Model utilizes the following principles:

Continuous creation of matter. A similar idea was proposed by Paul Dirac in 1974 [2]. According to WUM, the World is finite and is expanding inside the Universe which serves as an unlimited source of energy that continuously enters into the World.

Existence of the Medium of the World stated by Nikola Tesla: “*All attempts to explain the workings of the universe without recognizing the existence of the ether and the indispensable function it plays in the phenomena are futile and destined to oblivion*”. Unique properties of the Medium were discussed by James McCullagh in 1839. He proposed a theory of a rotationally elastic medium, i.e. a medium in which every particle resists absolute rotation. This theory produces equations analogous to Maxwell’s electromagnetic equations [11].

In WUM the World consists of the Medium (protons, electrons, photons, neutrinos, and dark matter particles) and Macroobjects (Galaxy clusters, Galaxies, Star clusters, Extrasolar systems, planets, etc.) made of these particles.

Decisive role of energy postulated by Nikola Tesla: “*There is no energy in matter other than that received from the environment*”.

Supremacy of matter postulated by Albert Einstein: “*When forced to summarize the theory of relativity in one sentence: time and space and gravitation have no separate existence from matter*”.

Principal role of Maxwell’s Equations (ME) that form the foundation of classical electrodynamics. The value of ME is even greater because J. Swain showed that “*linearized general relativity admits a formulation in terms of gravitoelectric and gravitomagnetic fields that closely parallels the description of the electromagnetic field by Maxwell’s equations*” [12]. Hans Thirring pointed out this analogy in his “On the formal analogy between the basic electromagnetic equations and Einstein’s gravity equations in first approximation” paper published in 1918 [13]. It allows us to use formal analogies between the electromagnetism and relativistic gravity. It is worth to note that *the equations for Gravitoelectromagnetism were first published in 1893, before general relativity, by Oliver Heaviside as a separate theory expanding Newton’s law* [Wikipedia, Gravitomagnetism].

In accordance with Maxwell’s equations for electromagnetism and gravitoelectromagnetism there are two measurable physical characteristics: energy density and energy flux density. For all particles under consideration we used four-momentum to conduct statistical analysis of particles’ ensembles with the final result – energy density.

Basic unit of energy density ρ_0 , basic unit of energy flux density I_0 , and basic unit of four-momentum p_0 are three measurable Fundamental Units of WUM. Two Fundamental Parameters in various rational exponents define all macro and micro features of the World: Fine-structure constant α and dimensionless quantity Q . While α is constant, Q increases with time, and is in fact a measure of the Size and the Age of the World [6].

This paper provides an overview of the World – Universe Model. The Model was developed in papers [3 – 10]. A number of results obtained there are quoted in the current work without a full justification; an interested reader is encouraged to view the referenced papers in such cases.

1. COSMOLOGY

WUM is built on two major assumptions: the universality of physical laws and the cosmological principle. The cosmological principle states that on large scale the World is homogeneous and isotropic. WUM envisions an expansion of the World.

1.1. THE BEGINNING AND EXPANSION

About 14.223 billion years ago the World was started by a fluctuation in the Universe, and the Nucleus of the World, which is a 4-ball, was born. The antipode length (the furthest distance between any two points) of the World's Nucleus at the Beginning was equal to

$$a = 2\pi a_0 \quad 1.1$$

where a_0 is the classical electron radius. The Nucleus has since been expanding through the Universe so that the antipode length is increasing with speed equal to the gravitoelectrodynamic constant c for cosmological time τ and has the length of $R = c\tau$. The corresponding diameter of the Nucleus D_N is: $D_N = 2R/\pi$.

The 4-ball is the interior of a 3-sphere which is the World in our Model. The 3-dimensional cubic hyperarea of a 3-sphere V_W is:

$$V_W = \frac{\pi^2}{4} D_N^3 = \frac{2}{\pi} R^3 \quad 1.2$$

The extrapolated energy density of the World at the Beginning is much smaller than the nuclear energy density [6, 7].

1.2. THE WORLD'S MATTER CONTENT

The World consists of the Medium (protons, electrons, photons, neutrinos, and dark matter particles) and Macroobjects (Galaxy clusters, Galaxies, Star clusters, Extrasolar systems, planets, etc.) made of these particles. There are no empty space and dark energy in the WUM.

1.3. HORIZON AND FLATNESS

The principal idea of WUM is that the energy density of the World ρ_W equals to the critical energy density ρ_{cr} necessary for a flat World at any cosmological time τ . The World is a closed structure. Hence the Horizon problem does not arise.

1.4. THE CREATION OF MATTER

Recall the well-known Friedmann equation for the critical energy density of the World ρ_{cr} :

$$\rho_{cr} = \frac{3H^2c^2}{8\pi G} \quad 1.3$$

where G is the gravitational parameter and H is Hubble's parameter:

$$H = \frac{1}{\tau} = \frac{c}{R} \quad 1.4$$

Equation 1.3 can be rewritten as

$$\frac{4\pi G}{c^2} \times \frac{2}{3} \rho_{cr} = \mu_g \times \frac{2}{3} \rho_{cr} = \mu_g \times \rho_M = H^2 = \frac{1}{\tau^2} = \frac{c^2}{R^2} \quad 1.5$$

where μ_g is the gravitomagnetic parameter and $\rho_M = \frac{2}{3} \rho_{cr}$ is the energy density of the Medium. According to Paul Dirac the gravitational parameter G is proportional to $\frac{1}{R}$ and is decreasing in time as $G \propto \frac{1}{\tau}$ [1]. It means that ρ_{cr} and ρ_M are also proportional to $\frac{1}{R}$ and are decreasing in time as $\rho_M = \frac{2}{3} \rho_{cr} \propto \frac{1}{\tau}$. In frames of WUM the critical energy density equals to

$$\rho_{cr} = 3\rho_0 \times Q^{-1} = 3\rho_0 \frac{a}{R} \quad 1.6$$

Amount of energy added to the World from the Universe dE_W is proportional to the increase of the hyperarea of the 3-sphere dV_W :

$$dV_W = \frac{6}{\pi} R^2 dR \quad 1.7$$

and the energy density of the Medium ρ_M which is the surface energy density of the Nucleus.

The total amount of the World energy at cosmological time τ is thus

$$E_W = \frac{12}{\pi} \rho_0 a \int_0^R r dr = \frac{6}{\pi} \rho_0 a R^2 = \frac{6}{\pi} \sigma_0 R^2 \quad 1.8$$

where constant σ_0 equals to

$$\sigma_0 = \rho_0 a \quad 1.9$$

The energy density of the World ρ_W is inversely proportional to the Nucleus antipode length R :

$$\rho_W = \frac{6\pi^3 \sigma_0 R^2}{2\pi^3 R^3} = 3 \frac{\sigma_0}{R} = \rho_{cr} \quad 1.10$$

and equals to ρ_{cr} necessary for the flat World at any cosmological time τ . It is important to note that:

- In our calculations we used the measurable Fundamental unit – energy density;
- Energy continuously enters from the Universe perpendicular to the 3-sphere and saturates all points of the World at the same time;
- Energy density of the World is the surface energy density of the Nucleus. The fluctuations of energy density in the World with the value higher than the energy density of the Medium are the fluctuations of 3-sphere surface energy density and correspond to “ripples, hills and bumps” of 3-sphere curved in a fourth dimension.

1.5. NEWTONIAN PARAMETER OF GRAVITATION

In accordance with WUM the parameter G can be calculated based on the value of the energy density of the Medium of the World ρ_M :

$$G = \frac{c^4}{8\pi\sigma_0 R} = \frac{\rho_M}{16\pi} \left(\frac{c^2}{\sigma_0}\right)^2 \quad 1.11$$

Then the Newton's law of universal gravitation can be rewritten in the following way:

$$F = G \frac{mM}{r^2} = \frac{\rho_M}{16\pi} \frac{\frac{mc^2 Mc^2}{\sigma_0}}{r^2} \quad 1.12$$

where we introduced the measurable parameter of the Medium ρ_M instead of the phenomenological coefficient G ; and gravitoelectromagnetic charges $\frac{mc^2}{\sigma_0}$ and $\frac{Mc^2}{\sigma_0}$ instead of macroobjects masses m and M . The gravitoelectromagnetic charges have a dimension of "area", which is equivalent to "energy", with the coefficient that equals to σ_0 .

In our Model, the gravitational parameter G can be calculated based on the value of H :

$$G = \frac{c^3}{8\pi\sigma_0} H \quad 1.13$$

Hubble's parameter H is the impedance of the Medium filled with matter. It follows that measuring the value of Hubble's parameter anywhere in the World and taking its inverse value allows us to calculate the absolute age of the World.

The gravitomagnetic parameter of the Medium μ_M equals to:

$$\mu_M = \frac{1}{R} \quad 1.14$$

Taking its inverse value, we can find the absolute size of the World. We emphasize that the above two parameters (H and μ_M) are principally different physical characteristics of the Medium that are connected through the gravitodynamic constant c .

In WUM, time and space are closely connected with the Medium's impedance and gravitomagnetic parameter. It follows that neither time nor space could be discussed in absence of the Medium. Matter, then, is primary to time and space. It follows that the gravitational parameter G can be introduced only for the World filled with matter, as Einstein has postulated.

While in our Model Hubble's parameter H has a clear physical meaning, the gravitational parameter G is a phenomenological coefficient in the Newton's law of universal gravitation and in Einstein's theory of general relativity.

1.6. TIME VARYING PARAMETERS OF THE WORLD

The constancy of the universe fundamental constants, including G , Fermi coupling constant G_F , Planck mass M_P , is now commonly accepted, although has never been firmly established as a fact. A commonly held opinion states that *gravity has no established relation to other fundamental forces*,

so it does not appear possible to calculate it indirectly from other constants that can be measured more accurately, as is done in some other areas of physics [Wikipedia, Gravitational constant].

WUM holds that there indeed exist relations between all Q -dependent, time varying parameters: G , G_F , M_P , H , R , ρ_{cr} , A_τ (Age of the World), T_{MBR} (Temperature of the microwave background radiation), m_{ph} (Photon rest mass), m_ν (Neutrino mass), etc. [3]. In accordance with WUM, the dimensionless quantity Q in various rational exponents defines all time varying parameters of the World as follows [3, 4]:

- Newtonian parameter of gravitation G

$$G = \frac{c^4}{8\pi\sigma_0 a} \times Q^{-1} \quad 1.15$$

- Hubble's parameter H

$$H = \frac{c}{a} \times Q^{-1} \quad 1.16$$

- Age of the World A_τ

$$A_\tau = \frac{a}{c} \times Q \quad 1.17$$

- Size of the World R

$$R = a \times Q \quad 1.18$$

- Critical energy density ρ_{cr}

$$\rho_{cr} = 3\rho_0 \times Q^{-1} \quad 1.19$$

- Planck mass

$$M_P = 2 \frac{E_0}{c^2} \times Q^{1/2} \quad 1.20$$

- Temperature of the microwave background radiation T_{MBR}

$$T_{MBR} = \frac{E_0}{k_B} \left(\frac{15\alpha m_e}{2\pi^3 m_p} \right)^{1/4} \times Q^{-1/4} \quad 1.21$$

- Temperature of the far-infrared background radiation peak T_{FIRB}

$$T_{FIRB} = \frac{E_0}{k_B} \left(\frac{15}{4\pi^5} \right)^{1/4} \times Q^{-1/4} \quad 1.22$$

- Fermi coupling parameter G_F

$$\frac{G_F}{(\hbar c)^3} = \left(1800 \alpha \frac{m_e}{m_p} \right)^{1/4} \frac{m_p}{m_e E_0^2} \times Q^{-1/4} \quad 1.23$$

where m_p is the mass of a proton, m_e is the mass of an electron, k_B is Boltzmann constant, α is the fine-structure constant, \hbar is Dirac constant, and the basic energy unit E_0 equals to [6]:

$$E_0 = \frac{p_0 l_0}{\rho_0} = p_0 c = \frac{\hbar c}{a} \quad 1.24$$

where h is Planck constant. Total energy of the World E_W at cosmological time τ equals to

$$E_W = \frac{6}{\pi} E_0 \times Q^2 = \frac{6}{\pi} E_0 \left(\frac{A_\tau}{t_0} \right)^2 \quad 1.25$$

where the basic unit of time t_0 equals to

$$t_0 = \frac{a}{c} \quad 1.26$$

The proportionality of total energy in the World to its age squared ($E_W \propto A_\tau^2$) was also hypothesized by Paul Dirac [1]. Using equation 1.15 we can find the dimensionless time varying fundamental parameter Q_G based on the average value of parameter G [4]:

$$Q_G = 0.760000(91) \times 10^{40} \quad 1.27$$

Today, Fermi coupling parameter G_F is known with the highest precision. Based on its average value we can calculate Q_F using equation 1.23:

$$Q_F = 0.759960(13) \times 10^{40} \quad 1.28$$

and significantly increase the precision of all Q -dependent parameters [4]. We propose to introduce Q as a new fundamental parameter tracked by CODATA, and use its value in calculation of all time-dependent parameters.

1.7. MACROOBJECTS OF THE WORLD. PIONEER ANOMALY

All macroobjects (MO) of the World (galaxy clusters, galaxies, star clusters, extrasolar systems, and planets) have cores made up of different Dark Matter (DM) particles (see Section 3.7). The theory of fermion compact stars made up of DM particles is well developed. Scaling solutions are derived for free and an interacting Fermi gas in [3]. The calculated parameters of fermion compact stars show that

- Strongly interacting WIMPs or neutralinos make up the cores of planets;
- White Dwarf Shells around the nuclei made of strongly interacting WIMPs or neutralinos compose the cores of stars in extrasolar systems;
- Monopoles (dissociated DIRACs) form cores of star clusters;
- Preons (dissociated ELOPs) constitute cores of galaxies;
- Sterile neutrinos make up cores of galaxy clusters.

According to the developed Model, Macroobjects have cores made up of fermionic DM particles possessing minimum radii R_{CORE} described in Tables 1 & 2 (Section 3.7). In case of extrasolar systems, the cores are made up of strongly interacting neutralinos or WIMPs surrounded with White Dwarf Shells (WDS).

The cores are surrounded by the transitional region. In this region, the density decreases rapidly to the point of the zero level of the fractal structure [14] characterized by radius R_f and energy density ρ_f that satisfy the following equation for $r \geq R_f$:

$$\rho(r) = \frac{\rho_f R_f}{r} \quad 1.29$$

According to Yu. Baryshev: “For a structure with fractal dimension $D = 2$ the constant $\rho_f R_f$ may be actually viewed as a new fundamental physical constant” [14]. In our Model, it is natural to connect this constant with the constant σ_0 :

$$\rho_f R_f = 4\sigma_0 \quad 1.30$$

The value of 4 above follows from the ratio for all Macroobjects of the World: 1/3 of the overall energy is in the central macroobject (for example, star in extrasolar system) and 2/3 of the energy is in the fractal structure around it [3].

It allows us to explain the so-called “Pioneer anomaly”. *The Pioneer anomaly is the observed deviation from predicted accelerations of the Pioneer 10 and Pioneer 11 spacecraft after they passed about 20 astronomical units (3×10^9 km; 2×10^9 mi) on their trajectories out of the Solar System. An unexplained force appeared to cause an approximately constant sunward acceleration of $a_p = 8.74 \pm 1.33 \times 10^{-10}$ m/s² for both spacecraft. The magnitude of the Pioneer effect a_p is numerically quite close to the product of the speed of light c and the Hubble constant H_0 hinting at cosmological connection.* [Wikipedia, Pioneer anomaly].

Let us calculate a deceleration a_p at the distance $r_p \gg R_f$ due to the additional mass of the fractal structure $M_{FS}(r_p) \propto r_p^2$ with the equation 1.14 for the gravitational parameter G :

$$a_p = \frac{GM_{FS}}{r_p^2} = \frac{c^4}{8\pi\sigma_0 R_0} \times 2\pi \frac{4\sigma_0}{c^2} = \frac{c^2}{R_0} = cH_0 = 6.68 \times 10^{-10} \text{ m/s}^2 \quad 1.31$$

which is in good agreement with the experimentally measured value (R_0 and H_0 are the values of R and H at the time of observation τ_0). It is important to notice that the calculated deceleration does not depend on r_p and equals to cH_0 hinting at cosmological connection. As for the values of R_f and ρ_f , let us take

$$R_f = \alpha^{-1} R_{CORE} \quad 1.32$$

$$\rho_f = 4\sigma_0 \frac{\alpha}{R_{CORE}} \quad 1.33$$

Equation 1.29 fits naturally into our Model, since the evolution of all spherical structures of the World is progressing in a quasi-stationary mode. The ball of radius R_f is receiving energy from the Universe, and the distribution of energy outside of the ball follows equation 1.29.

The calculations carried out for our Sun using equations 1.32 and 1.33 are in agreement with the experimentally measured characteristics of the Sun. Taking the value of the solar core radius $R_{CORESun} \cong 1.6 \times 10^8$ m (see 2.14.16 in [3]) we obtain

$$R_f \cong 2.2 \times 10^{10} \text{ m} \quad 1.34$$

which is in agreement with estimated size of the Heliosphere. *The Heliosphere, which is the cavity around the Sun filled with the solar wind plasma, extends from approximately 20 solar radii ($\sim 1.4 \times 10^{10} \text{ m}$) to the outer fringes of the Solar System* [Wikipedia, Sun].

Mass of the fractal structure around Sun M_V at distances $R_V \gg R_f$ is

$$M_V = 8\pi R_V^2 \sigma_0 / c^2 \quad 1.35$$

At distance $R_V = 1.8 \times 10^{13} \text{ m}$ away from the Sun (approximate distance to Voyager 1 [125]),

$$M_V \cong 3.3 \times 10^{27} \text{ kg} \quad 1.36$$

that is $\sim 0.15\% M_{Sun}$. This additional mass can explain the observed deceleration of Voyagers.

1.8. NUCLEOSYNTHESIS

Nucleosynthesis of all elements (including light elements) occurs inside stars during their evolution (Stellar nucleosynthesis). The theory of this process is well developed, starting with the publication of a celebrated B²FH review paper in 1957 [15]. With respect to WUM, stellar nucleosynthesis theory should be enhanced to account for annihilation of heavy Dark Matter particles (WIMPs and neutralinos). The amount of energy produced due to this process is sufficiently high to produce all elements inside stellar cores.

1.9. COSMOLOGICAL REDSHIFT

WUM gives the following explanations for supernovae Ia distance measurements and their relation to redshift: all macroobjects of the World were fainter in the past. As their cores absorb new energy, the size of macroobjects R_{MO} and their luminosity L_{MO} are increasing in time $R_{MO} \propto Q^{1/2} \propto \tau^{1/2}$ and $L_{MO} \propto Q \propto \tau$ correspondingly. For example, taking the age of the World $\cong 14.2 \text{ Byr}$ and the age of solar system $\cong 4.6 \text{ Byr}$, it is easy to find that the young Sun's output was 67.6% of what it is today. Literature commonly refers to the value of 70% [126].

Interestingly, Nikola Tesla shared the same opinion. In 1934, “*Dr. Tesla disclosed that he has lately perfected instruments which flatly disprove the present theory of the high physicists that the sun is destined to burn itself out until it is a cold cinder floating in space. Dr. Tesla stated that he is able to show that all the suns in the universe are constantly growing in mass and heat, so that the ultimate fate of each is explosion*” [16].

In accordance with Hubble's law, a distance d to galaxy for $z \ll 1$ is found to be proportional to z :

$$d = \frac{c}{H} z = Rz \quad 1.37$$

The relationship of distance d to the redshift z for large values of z is not presently conclusive, active research is conducted in the area. In WUM, the distance to galaxy equals to

$$d = \frac{c}{H} \frac{z}{1+z} = R \frac{z}{1+z} \quad 1.38$$

which reduces to 1.37 for $z \ll 1$ and $d = R$ for $z \rightarrow \infty$. Thus for $z > 1$, the distance to supernovae is smaller than expected and hence supernovae are brighter. There is then no reason to introduce dark energy in order to explain the nonlinear relationship of distance to the redshift.

2. COMPARING WORLD – UNIVERSE MODEL AND BIG BANG MODEL

Let's proceed to compare the origin, evolution, structure, ultimate fate, and parameters of the World speculated by the Big Bang Model (BBM) and World – Universe Model (WUM).

2.1. THE BEGINNING AND EXPANSION

BBM: *"About 13.772 billion years (Byr) ago a tremendous explosion started the expansion of the universe. This explosion is known as the Big Bang. At the point of this event all of the matter and energy of space was contained at one point (singularity). What existed prior to this event is completely unknown and is a matter of pure speculation. This occurrence was not a conventional explosion but rather an event filling all of space with all of the particles of the embryonic universe rushing away from each other. The Big Bang actually consisted of an explosion of space within itself unlike an explosion of a bomb where fragments are thrown outward"* [127].

Inflationary Epoch lasted from 10^{-36} to approximately 10^{-32} seconds after the Big Bang. Universe underwent an extremely rapid exponential expansion. This rapid expansion increased the linear dimensions of the early universe by a factor of at least 10^{26} (and possibly a much larger factor), and so increased its volume by a factor of at least 10^{78} . This expansion explains various properties of the current universe that are difficult to account for without such an inflationary epoch (Horizon and Flatness problems). Following the inflationary period, the universe continued to expand, but at a slower rate [Wikipedia, Inflationary epoch].

WUM: About 14.223 billion years ago the World was started by a fluctuation in the Universe, and the 4-ball Nucleus of the World with the antipode length a was born (1.1). The extrapolated energy density of the 3-sphere World at the Beginning was

$$\rho_{W0} = 3\rho_0 = 6.0638901 \times 10^{30} \frac{J}{m^3} \quad 2.1$$

which is four orders of magnitude smaller than the nuclear energy density (see equation 3.7.1). The Nucleus has since been expanding through the Universe so that the antipode length is increasing with speed equal to the gravitoelectrodynamic constant c .

2.2. THE SIZE AND AGE OF THE WORLD

BBM: *Current interpretations of astronomical observations indicate that the age of the Universe is 13.772 Byr (the Hubble radius equals to 13.772 billion light years) and that the diameter of the observable universe is at least 93 billion light years. According to general relativity, space can expand faster than the speed of light, although we can view only a small portion of the universe due to the limitation imposed by light speed. Since we cannot observe space beyond the limitations of light (or any electromagnetic radiation), it is uncertain whether the size of the Universe is finite or infinite* [Wikipedia, Universe].

WUM: According to the Model, the 3-spere World is a closed structure. The antipode length of the 4-ball Nucleus equals to the Hubble radius (about 14.223 Byr).

2.3. HORIZON AND FLATNESS

BBM: *The horizon problem is the problem of determining why the universe appears statistically homogeneous and isotropic in accordance with the cosmological principle. In the big bang model without inflation gravitational expansion does not give the early universe enough time to equilibrate. In a big bang with only the matter and radiation known in the Standard Model, two widely separated regions of the observable universe cannot have equilibrated because they move apart from each other faster than the speed of light – thus have never come in to causal contact: in the history of the universe, back to the earliest times, it has not been possible to send a light signal between the two regions. Because they have no interaction, it is difficult to explain why they have the same temperature (are thermally equilibrated) [Wikipedia, Inflation (cosmology)].*

WUM: The energy density of the World equals to the critical energy density necessary for a flat World. The World is a closed structure. Hence the Horizon problem does not arise.

2.4. THE CREATION OF MATTER

BBM: At the point of the Big Bang all of the matter and energy of space was contained at one point.

WUM: Creation of all matter in the World continually occurs by receiving energy from the Universe.

2.5. NEWTONIAN PARAMETER OF GRAVITATION

BBM: Newtonian constant of gravitation G is a Fundamental constant.

WUM: The gravitational parameter G is decreasing in time as $G \propto \frac{1}{\tau}$.

2.6. NUCLEOSYNTHESIS

BBM: *It is now known that the elements observed in the Universe were created in either of two ways. Light elements (namely deuterium, helium, and lithium) were produced in the first few minutes of the Big Bang, while elements heavier than helium are thought to have their origins in the interiors of stars which formed much later in the history of the Universe. Both theory and observation lead astronomers to believe this to be the case. The measured abundances all agree at least roughly with those predicted by the Big Bang model from a single value of the baryon-to-photon ratio. The agreement is excellent for deuterium, close but formally discrepant for ${}^4\text{He}$, and off by a factor of two for ${}^7\text{Li}$; in the latter two cases there are substantial systematic uncertainties. Nonetheless, the general consistency with abundances predicted by Big Bang nucleosynthesis is strong evidence for the Big Bang [Wikipedia, Big Bang Nucleosynthesis].*

WUM: Nucleosynthesis of all elements including light elements occurs inside stars during their evolution (Stellar nucleosynthesis).

2.7. MICROWAVE BACKGROUND RADIATION

BBM: *About 380,000 years after the Big Bang the temperature of the universe fell to the point where nuclei could combine with electrons to create neutral atoms. As a result, photons no longer interacted*

frequently with matter, the universe became transparent and the cosmic microwave background radiation was created and then structure formation took place. This cosmic event is usually referred to as decoupling. The photons present at the time of decoupling are the same photons that we see in the cosmic microwave background radiation, after being greatly cooled by the expansion of the Universe. The photons that existed at the time of photon decoupling have been propagating ever since, though growing fainter and less energetic, since the expansion of space causes their wavelength to increase over time [Wikipedia, Cosmic microwave background radiation].

WUM: The black body spectrum of the cosmic microwave background radiation (MBR) is due to thermodynamic equilibrium of photons with low density intergalactic plasma. The World – Universe Model calculates the value of MBR temperature $T_{MBR} = 2.72522\text{ K}$, that is in excellent agreement with experimentally measured value of $2.72548 \pm 0.00057\text{ K}$ [Wikipedia, Cosmic microwave background radiation].

2.8. FORMATION AND EVOLUTION OF LARGE-SCALE STRUCTURES

BBM: Cosmologists study a model of hierarchical structure formation in which structures form from the bottom up, with smaller objects forming first, while the largest objects, such as superclusters, are still assembling. *A combination of observations and theory suggest that the first quasars and galaxies formed about a billion years after the Big Bang, and since then larger structures have been forming, such as galaxy clusters and superclusters. Populations of stars have been aging and evolving, so that distant galaxies (which are observed as they were in the early Universe) appear very different from nearby galaxies (observed in a more recent state)* [Wikipedia, Big Bang].

WUM: All macroobjects of the World have cores made up of different DM particles. The energy consumption rates are greater for galaxies relative to extrasolar systems, and for the World relative to galaxies. It follows that new stars and star clusters can be created inside of a galaxy, and new galaxies and galaxy clusters can arise in the World. Structures form from top (the World) down to extrasolar systems in parallel around different cores made of different DM particles. Formation of galaxies and stars is not a process that concluded ages ago; instead, it is ongoing.

2.9. COSMOLOGICAL REDSHIFT. DARK ENERGY

BBM: *Hubble's law of the correlation between redshifts and distances is required by models of cosmology derived from general relativity that have a metric expansion of space. As a result, photons propagating through the expanding space are stretched, creating the cosmological redshift* [Wikipedia, Redshift].

In physical cosmology and astronomy, dark energy is a hypothetical form of energy that permeates all of space and tends to accelerate the expansion of the universe. Of particular importance are the observations that extremely high red shift ($z > 1$) supernovae are brighter than expected. [Wikipedia, Physical cosmology].

WUM: The World – Universe model gives the following explanation for supernovae Ia distance measurements: the distance to galaxies equals to

$$d = \frac{c}{H} \frac{z}{1+z} = R \frac{z}{1+z} \quad 2.2$$

which reduces to 1.37 for $z \ll 1$ and $d = R$ for $z \rightarrow \infty$. Thus for $z > 1$, the distance to supernovae is smaller than expected and hence supernovae are brighter. There is then no reason to introduce dark energy.

2.10. ULTIMATE FATE OF THE UNIVERSE

BBM: *There's a growing consensus among cosmologists that the universe is flat and will continue to expand forever. The preponderance of evidence to date, based on measurements of the rate of expansion and the mass density, favors a universe that will continue to expand indefinitely, resulting in the "big freeze" scenario below. However, observations are not conclusive, and alternative models are still possible. The Big Freeze is a scenario under which continued expansion results in a universe that asymptotically approaches absolute zero temperature. A related scenario is heat death, which states that the universe goes to a state of maximum entropy in which everything is evenly distributed, and there are no gradients – which are needed to sustain information processing, one form of which is life* [Wikipedia, Ultimate fate of the universe].

WUM: The World is continuously receiving energy from the Universe that envelopes it. Assuming an unlimited Universe, the numbers of cosmological structures on all levels will increase: new galaxy clusters will form; existing clusters will obtain new galaxies; new stars will be born inside existing galaxies; sizes of individual stars will increase, etc. The temperature of the Medium of the World will asymptotically approach absolute zero (Section 3.2).

3. ASTROPARTICLE PHYSICS

3.1. BASIC UNIT OF MASS

More than 60 years ago, Y. Nambu proposed an empirical mass spectrum of elementary particles with a mass unit close to one quarter of the mass of a pion (about $\frac{m_0}{2} \cong 35 \text{ MeV}/c^2$) [17]. He noticed that meson masses are even multiples of a mass unit $\frac{m_0}{2}$, baryon (and also unstable lepton) masses are odd multiples, and mass differences among similar particles are quantized by $m_0 \cong 70 \text{ MeV}/c^2$. During the last 40 years M. Mac Gregor studied this property extensively [18].

In WUM we introduced a basic unit of mass m_0 that equals to

$$m_0 = \frac{\hbar}{ac} = 70.025267 \text{ MeV}/c^2 \quad 3.1.1$$

3.2. LOW DENSITY PLASMA. TEMPERATURE OF THE MICROWAVE BACKGROUND RADIATION

In our Model, the World consists of stable elementary particles with lifetimes longer than the age of the World. Protons and electrons have identical concentrations in the Medium of the World [3]:

$$n_p = n_e = \frac{2\pi^2 m_e}{a^3 m_p} \times Q^{-1} = 0.25480 \text{ m}^{-3} \quad 3.2.1$$

which is in good agreement with their estimated concentration in the intergalactic medium $n_p \cong 0.25 \text{ m}^{-3}$ [Wikipedia, Outer space]. Low density plasma has plasma frequency ν_{pl} [3]:

$$\nu_{pl} = \frac{c}{a} \left(\frac{m_e}{m_p} \right)^{1/2} \times Q^{-1/2} = 4.5322 \text{ Hz} \quad 3.2.2$$

Photons with energy smaller than $E_{ph} = h\nu_{pl}$ cannot propagate in plasma, thus $h\nu_{pl}$ is the smallest amount of energy a photon may possess (Section 3.3). $\rho_p = n_p E_p$ is the energy density of protons in the Medium. The relative energy density of protons Ω_p is then the ratio of $\frac{\rho_p}{\rho_{cr}}$:

$$\Omega_p = \frac{\rho_p}{\rho_{cr}} = \frac{2\pi^2 \alpha}{3} = 0.048014655 \quad 3.2.3$$

The above value is in a good agreement with estimations of baryonic matter in the World $\Omega_p \cong 0.046$ [Wikipedia, Dark Matter]. $\rho_e = n_e E_e$ is the energy density of electrons in the Medium. The relative energy density of electrons Ω_e is then the ratio of $\frac{\rho_e}{\rho_{cr}}$:

$$\Omega_e = \frac{\rho_e}{\rho_{cr}} = \frac{2\pi^2 \alpha}{3} \frac{m_e}{m_p} \quad 3.2.4$$

Let's assume that the energy density of MBR ρ_{MBR} is twice larger than ρ_e (due to two polarizations of photons):

$$\rho_{MBR} = 4\pi^2 \alpha \frac{m_e}{m_p} \rho_0 \times Q^{-1} = \frac{8\pi^5}{15} \frac{k_B^4}{(hc)^3} T_{MBR}^4 \quad 3.2.5$$

where T_{MBR} is MBR temperature. The black body spectrum of MBR is due to thermodynamic equilibrium of photons with intergalactic plasma. We can now calculate the value of T_{MBR} :

$$T_{MBR} = \frac{E_0}{k_B} \left(\frac{15\alpha m_e}{2\pi^3 m_p} \right)^{1/4} \times Q^{-1/4} = 2.72522 \text{ K} \quad 3.2.6$$

Thus calculated value of T_{MBR} is in excellent agreement with experimentally measured value of $2.72548 \pm 0.00057 \text{ K}$ [Wikipedia, Cosmic microwave background radiation].

3.3. MASS VARYING PHOTONS. SPEED OF LIGHT

Photons with energy smaller than $E_{ph} = h\nu_{pl}$ cannot propagate in plasma, thus $h\nu_{pl}$ is the smallest amount of energy a photon may possess. This amount of energy can be viewed as a particle (we will name it axion), whose frequency-independent effective “rest mass” equals to [3]:

$$m_a = m_0 \left(\frac{m_e}{m_p} \right)^{1/2} \times Q^{-1/2} = 1.8743 \times 10^{-14} \text{ eV}/c^2 \quad 3.3.1$$

The calculated mass of an axion is in agreement with $m_a \sim 10^{-15} \text{ eV}/c^2$ discussed by C. Csaki *et al.* [19] and with experimental checks of Coulomb's law on photon mass m_{ph} . A null result of such an experiment has set a limit of $m_{ph} \lesssim 10^{-14} \text{ eV}/c^2$. If the photon mass is generated via the Higgs

mechanism then the upper limit of $m_{ph} \lesssim 10^{-14} \text{ eV}/c^2$ from the test of Coulomb's law is valid [Wikipedia, Photon].

According to special relativity, energy of an axion E_a moving with a group velocity v_{gr} is given by

$$E_a(v_{gr}) = h\nu_{pl}(1 - \frac{v_{gr}^2}{c^2})^{-1/2} \quad 3.3.2$$

Taking into account the dispersion relation for plasma:

$$v_{gr}\nu_{ph} = c^2 \quad 3.3.3$$

and the value of phase velocity $\nu_{ph} = \frac{c}{n_{pl}}$, where n_{pl} is the index of plasma refraction

$$n_{pl} = (1 - \frac{\nu_{pl}^2}{\nu^2})^{1/2} \quad 3.3.4$$

we calculate moving axion energy $E_a(v_{gr})$ to be

$$E_a(v_{gr}) = h\nu = E_{ph} \quad 3.3.5$$

where ν is photon frequency.

In our Model, the total energy of a moving particle consists of two components: rest energy and "coat" energy. A particle's coat is the response of the Medium to the particle's movement. A photon is then a constituent axion with rest energy $E_a = h\nu_{pl}$ and total energy $E_{ph} = h\nu$. In most cases, $\nu \gg \nu_{pl}$, and practically all of the photon's energy is concentrated in the axion's coat that is part of the Medium surrounding the axion. Axions are fully characterized by their four-momentum.

Rest energy of an axion is decreasing with time: $E_a \propto \tau^{-1/2}$ (3.3.1), and total energy remains constant in the ideal frictionless Medium. The higher the photon's energy, the closer its speed approaches c . But the fact that axions possess non-zero rest masses means that photons can never reach that speed.

3.4. MASS VARYING NEUTRINOS

It is now established that there are three different types of neutrinos: electronic ν_e , muonic ν_μ , and tauonic ν_τ , and their antiparticles. Pontecorvo and Smorodinskii discussed the possibility of energy density of neutrinos exceeding that of baryonic matter [20]. Neutrino oscillations imply that neutrinos have non-zero masses.

In WUM, neutrino masses are related to and proportional to m_0 multiplied by fundamental parameter $Q^{-1/4}$ and different coefficients that were found in [3]. Masses of neutrinos are predicted as follows:

$$m_{\nu_e} = \frac{1}{24} m_0 \times Q^{-1/4} = 3.1250 \times 10^{-4} \text{ eV}/c^2 \quad 3.4.1$$

$$m_{\nu_\mu} = m_0 \times Q^{-1/4} = 7.4999 \times 10^{-3} \text{ eV}/c^2 \quad 3.4.2$$

$$m_{\nu_\tau} = 6m_0 \times Q^{-1/4} = 4.5000 \times 10^{-2} \text{ eV}/c^2 \quad 3.4.3$$

The squared values of the muonic and tauonic masses fall into the ranges of mass splitting Δm_{sol}^2 and Δm_{atm}^2 for solar and atmospheric neutrinos respectively estimated in literature [3]. The sum of the calculated neutrino masses

$$\Sigma m_\nu \cong 0.053 \text{ eV}/c^2 \quad 3.4.4$$

is in good agreement with the value of $0.06 \text{ eV}/c^2$ discussed in literature [21].

One of the principal ideas of the World – Universe Model holds that energy densities of Medium particles are proportional to proton energy density in the World's Medium (3.2.3). Therefore the total neutrinos relative energy density $\Omega_{\nu tot}$ (in the Medium and in macroobjects) in terms of the critical energy density ρ_{cr} equals to [3]:

$$\Omega_{\nu tot} = \frac{45}{\pi} \Omega_p = 30\pi\alpha = 0.68775927 \quad 3.4.5$$

3.5. COSMIC FAR-INFRARED BACKGROUND

3.5.1. INTRODUCTION

Cosmic infrared background (CIB) is a mysterious infrared light coming from outer space. It is slowly being resolved into specific sources by infrared telescopes. In some ways it is analogous to the cosmic microwave background, but at shorter wavelengths.

One of the most important questions about the CIB is the source of its energy. Dust in the host galaxies can absorb starlight and re-emit it in the infrared, contributing to the CIB. Although most of today's galaxies contain little dust (e. g. elliptical galaxies are practically dustless), there are some special stellar systems even in our vicinity which are extremely bright in the infrared and at the same time faint (often almost invisible) in the optical. These ultra-luminous infrared galaxies are just in a very active star formation period [Wikipedia, Cosmic Infrared background].

The cosmic Far-Infrared Background (FIRB), which was announced in January 1998, is the part of the CIB with wavelengths near 100 microns that is the peak power wavelength of the black body radiation at 29 K. Below we are going to introduce a new component of the Medium of the World – Bose-Einstein Condensate (BEC) drops of dineutrinos whose mass about equals to Planck mass, and their temperature is around 29 K. These drops are responsible for the FIRB.

3.5.2. OBSERVATIONS

The Infrared Astronomical Satellite (IRAS) was the first all-sky survey which used far-infrared wavelengths in 1983. Using IRAS, scientists were able to determine the luminosity of the galactic objects discovered. Over 250,000 infrared sources were observed during the 10 month mission.

The FIRB radiation was observed for different galaxies in [22-41]. M. G. Hauser *et al.* revealed bright emission from interplanetary dust at 100 micrometer [22]. F. J. Low *et al.* pointed out that the 100 micrometer cirrus may represent cold material in the outer solar system or a new component of the interstellar medium [23].

B. Wang in 1991 found that the integrated far-Infrared background (FIRB) from galaxies peaks at around 100 – 130 microns, with total radiation density from 0.5% to 6% of the cosmic MBR [24]. E. L. Wright in 1999 made the recomputation of the FIRB and found its total intensity to be about 3.4% of the MBR intensity [25].

In 1999, G. Lagache et al. described the Cosmic FIRB and announced that “*for the first time the far-IR emission of dust associated with the Warm Ionized Medium (WIM) is evidenced. The best representation of the WIM dust spectrum is obtained for a temperature of 29.1 K*” [30]. D. P. Finkbeiner et al. have detected substantial flux in the 60 and 100 micron channels in excess of expected zodiacal and Galactic emission. They concluded that “*there is currently no satisfactory explanation for the 60-100 micron excess*” [31].

M. J. Devlin et al. have this to say about a population of luminous, high-redshift, dusty starburst galaxies: “*In the redshift range $1 \leq z \leq 4$, these massive submillimeter galaxies go through a phase characterized by optically obscured star formation at rates several hundred times that in the local Universe. Half of the starlight from this highly energetic process is absorbed and thermally reradiated by clouds of dust at temperatures near 30 K with spectral energy distributions peaking at 100 μm* ” [38].

3.5.3. MODEL

According to WUM [3], the size of large cosmic grains D_G is roughly equal to the Fermi length L_F :

$$D_G \sim L_F = a \times Q^{1/4} = 1.6532 \times 10^{-4} \text{ m} \quad 3.5.1$$

and their mass m_G is close to the Planck mass M_P :

$$m_G \sim (10^{-9} \Leftrightarrow 10^{-7}) \text{ kg} \quad 3.5.2$$

The density of grains ρ_G is close to the rock density ρ_{rock} :

$$\rho_G \sim \rho_{rock} = \frac{6 M_P}{\pi L_F^3} = 9.2008 \times 10^3 \frac{\text{kg}}{\text{m}^3} \quad 3.5.3$$

According to WUM, Planck mass M_P equals to

$$M_P = 2m_0 \times Q^{1/2} \quad 3.5.4$$

Note that the value of M_P is increasing with cosmological time, and is proportional to $\tau^{1/2}$. Then,

$$\frac{d}{d\tau} M_P = \frac{M_P}{2\tau} \quad 3.5.5$$

A grain of mass $B_1 M_P$ and radius $B_2 L_F$ is receiving energy from the Medium of the World at the following rate:

$$\frac{d}{d\tau} (B_1 M_P c^2) = \frac{B_1 M_P c^2}{2\tau} \quad 3.5.6$$

where B_1 and B_2 are parameters.

The received energy will increase the grain's temperature T_G , until equilibrium is achieved: power received equals to the power irradiated by the surface of a grain in accordance with the Stefan-Boltzmann law

$$\frac{B_1 M_P c^2}{2\tau} = \sigma_{SB} T_G^4 \times 4\pi B_2^2 L_F^2 \quad 3.5.7$$

where σ_{SB} is Stefan-Boltzmann constant:

$$\sigma_{SB} = \frac{2\pi^5 k_B^4}{15 h^3 c^3} \quad 3.5.8$$

With Nikola Tesla's principle at heart – *There is no energy in matter other than that received from the environment* – we apply the World equation [3] to a grain:

$$B_1 M_P c^2 = 4\pi B_2^2 L_F^2 \sigma_0 \quad 3.5.9$$

We then calculate the grain's stationary temperature T_G to be

$$T_G = \left(\frac{15}{4\pi^5}\right)^{1/4} \frac{hc}{k_B L_F} = 28.955 K \quad 3.5.10$$

This result is in an excellent agreement with experimentally measured value of 29 K [30-41].

3.5.4. RELATION TO MICROWAVE BACKGROUND

WUM calculates the value of the microwave background radiation temperature T_{MBR} to be:

$$T_{MBR} = \left(\frac{15\alpha m_e}{2\pi^3 m_p}\right)^{1/4} \frac{hc}{k_B L_F} = 2.72522 K \quad 3.5.11$$

Comparing equations 3.5.10 and 3.5.11, we can find the relation between the grains' temperature and the temperature of the microwave background radiation:

$$T_G = (3\Omega_e)^{-1/4} \times T_{MBR} = 28.955 K \quad 3.5.12$$

Cosmic FIRB radiation is not black body radiation. Otherwise, its energy density ρ_{FIRB} at temperature T_G would equal to the energy density of the Medium of the World:

$$\rho_{FIRB} = \frac{8\pi^5}{15} \frac{k_B^4}{(hc)^3} T_G^4 = \frac{2}{3} \rho_{cr} = \rho_M \quad 3.5.13$$

The total flux of the FIRB radiation is the sum of the contributions of all individual grains.

3.5.5. PLANCK MASS

The developed model of the FIRB introduces large grains whose mass about equals to Planck mass M_P . Recall Dirac's quantization condition:

$$\frac{e\mu}{4\pi\epsilon_0} = n \frac{hc}{4\pi} \quad 3.5.14$$

where n is an integer, ϵ_0 is the electric parameter, e and μ are electron and Dirac's monopole charges respectively.

Taking into account the analogy between electromagnetic and gravitoelectromagnetic fields, we can rewrite the same equation for masses of a gravitoelectromagnetic field:

$$\frac{mM}{4\pi\epsilon_g} = \frac{hc}{2\pi} \frac{mM}{M_P^2} = n \frac{hc}{4\pi} \quad 3.5.15$$

where ϵ_g is the gravitoelectric parameter. Taking $n = 1$ we obtain the minimum product of masses

$$mM = \frac{1}{2} M_P^2 = 2.36904 \times 10^{-16} \text{ kg}^2 \quad 3.5.16$$

Two particles or microobjects will not exert gravity on one another when both of their masses are smaller than the Planck mass. Planck mass can then be viewed as the mass of the smallest macroobject capable of generating the gravitoelectromagnetic field, and serves as a natural borderline between classical and quantum physics. Incidentally, in his "Interpreting the Planck mass" paper, B. Hammel showed that the Plank mass is "*a lower bound on the regime of validity of General Relativity*" [42].

In our opinion, cosmic large grains with mass around M_P are the smallest building blocks of all macroobjects. Since these grains possess Planck mass, they can be reasoned about from the standpoint of classical physics, validating our calculations of the grains' masses and temperature.

3.5.6. MASS VARYING QUANTS. AXIONS AND DINEUTRINOS

According to WUM, all "elementary" particles of the World are fermions and they possess masses. Bosons such as photons, X-rays, and gamma rays are composite particles and consist of an even numbers of fermions. An axion is a boson possessing the lowest mass $m_a \sim 10^{-14} \text{ eV}/c^2$ (3.3.1).

Gamma rays are usually distinguished from X-rays by their origin: *X-rays are emitted by electrons outside the nucleus, while gamma rays are emitted by the nucleus* [Wikipedia, Gamma ray]. A better way to distinguish the two, in our opinion, is the type of fermions composing the core of X-quants and Gamma-quants.

Super soft X-rays have energies in the 0.09 to 2.5 keV range, whereas soft Gamma rays have energies in the 10 to 5000 keV range. We assume that X-quants are dineutrinos $\nu\bar{\nu}$ with the rest mass m_X (see Section 3.5.8):

$$m_X \propto m_0 \times Q^{-1/4} \sim 10^{-4} \text{ eV}/c^2 \quad 3.5.17$$

which is 10 orders of magnitude larger than the axion mass and is decreasing in time: $m_X \propto \tau^{-1/4}$. We will name these dineutrinos “Xions”. New Physics with the dineutrinos in the Rare Decay $B \rightarrow K\nu\bar{\nu}$ is actively discussed in literature in recent years (see, for example [43, 44]).

According to WUM, the total neutrinos energy density in the World is almost 10 times greater than baryonic energy density, and about 3 times greater than Dark Matter energy density (Section 3.5.7). At such a high neutrino concentration, “neutrinos pairs” $\nu\bar{\nu}$ (Xions) can be created. The concentration of Xions may indeed be sufficient to undergo Bose-Einstein condensation (BEC), and as a result create BEC drops (large grains), possessing masses roughly equal to Planck mass.

3.5.7. ENERGY DENSITY OF DINEUTRINOS AND FIRB

Our Model holds that the energy densities of all types of Dark Matter (DM) particles are proportional to the proton energy density ρ_p in the World’s Medium (3.2.3).

In all, there are 5 different types of DM particles (see Section 3.6). Then the total energy density of DM ρ_{DM} is

$$\rho_{DM} = 5\rho_p = 0.24007327\rho_{cr} \quad 3.5.18$$

which is close to the DM energy density discussed in literature: $\rho_{DM} \approx 0.23 \rho_{cr}$ [Wikipedia, Dark Matter].

The total neutrino energy density $\rho_{\nu tot}$ equals to

$$\rho_{\nu tot} = \frac{45}{\pi} \rho_p \quad 3.5.19$$

The total baryonic energy density ρ_B is:

$$\rho_B = 1.5\rho_p \quad 3.5.20$$

The sum of electron and MBR energy densities ρ_{eMBR} equals to

$$\rho_{eMBR} = \rho_e + \rho_{MBR} = 1.5 \frac{m_e}{m_p} \rho_p + 2 \frac{m_e}{m_p} \rho_p = 3.5 \frac{m_e}{m_p} \rho_p \quad 3.5.21$$

We took additional energy density ρ_{ADD}

$$\rho_{ADD} = \left(2 + \frac{1}{5\pi}\right) \frac{m_e}{m_p} \rho_p \quad 3.5.22$$

so that the energy density of the World ρ_W equals to the theoretical critical energy density ρ_{cr}

$$\rho_W = \left[\frac{13}{2} + \left(\frac{11}{2} + \frac{1}{5\pi} \right) \frac{m_e}{m_p} + \frac{45}{\pi} \right] \rho_p = \rho_{cr} \quad 3.5.23$$

From 3.5.23 we can calculate the value of the fine-structure constant α , using electron-to-proton mass ratio

$$\frac{1}{\alpha} = \frac{\pi}{15} \left[450 + 65\pi + (55\pi + 2) \frac{m_e}{m_p} \right] = 137.03600 \quad 3.5.24$$

which is in an excellent agreement with the commonly adopted value of 137.035999074(44).

It follows that there is a direct correlation between constants α and $\frac{m_e}{m_p}$ expressed by equation of the total energy density of the World (3.5.23). As shown above, $\frac{m_e}{m_p}$ is not an independent constant, but is instead derived from α . In Section 3.5.8 we will connect the chosen value of ρ_{ADD} with energy density of dineutrinos and FIRB radiation.

3.5.8. BOSE-EINSTEIN CONDENSATE

New cosmological models employing the Bose-Einstein Condensates (BEC) are actively discussed in literature in recent years [45-59].

The transition to BEC occurs below a critical temperature T_c , which for a uniform three-dimensional gas consisting of non-interacting particles with no apparent internal degrees of freedom is given by [Wikipedia, Bose-Einstein condensate]:

$$T_c = [\zeta(3/2)]^{-2/3} \frac{h^2 n_X^{2/3}}{2\pi m_X k_B} \approx \frac{h^2 n_X^{2/3}}{11.918 m_X k_B} \quad 3.5.25$$

where n_X is the particle density, m_X is the mass per boson, ζ is the Riemann zeta function:

$$\zeta(3/2) \approx 2.6124 \quad 3.5.26$$

According to our Model, we can take the value of the critical temperature T_c to equal the stationary temperature T_G of large grains (see equation 3.5.10). Let's assume that the energy density of boson particles ρ_X equals to the MBR energy density (see equation 3.2.5):

$$\rho_X = n_X m_X = 2 \frac{m_e}{m_p} \rho_p = 4\pi^2 \alpha \frac{m_e h c}{m_p L_F^4} = 0.00015690 \times \frac{hc}{L_F^4} \quad 3.5.27$$

Taking into account equations 3.5.10, 3.5.25 and 3.5.27, we can calculate the value of n_X :

$$\begin{aligned} n_X &= [47.672 \pi^2 \alpha \frac{m_e}{m_p} \left(\frac{15}{4\pi^5} \right)^{1/4}]^{3/5} \times L_F^{-3} = \\ &= 0.011922 \times L_F^{-3} = 2.6386 \times 10^9 \text{ m}^{-3} \end{aligned} \quad 3.5.28$$

and the value of the mass m_X :

$$m_X = \frac{\rho_X}{n_X c^2} = 0.013161 m_0 \times Q^{-1/4} = 0.987 \times 10^{-4} \text{ eV/c}^2 \quad 3.5.29$$

m_X is 10 orders of magnitude larger than the axion mass (see equation 3.3.1).

The calculated values of the mass and concentration of dineutrinos satisfy the conditions for their Bose-Einstein condensation. Consequently, BEC drops whose masses about equal to Planck mass can be created. The stability of such drops is provided by the discussed detailed equilibrium

between the energy absorption from the Medium of the World and re-emission of this energy in FIRB at the stationary temperature $T_G = 29 K$.

The FIRB energy density ρ_{FIRB} equals to

$$\rho_{FIRB} = \rho_{ADD} - \rho_X = \frac{1}{5\pi m_p} \frac{m_e}{m_p} \rho_p \quad 3.5.30$$

which is 10π times smaller than the energy density of MBR and dineutrinos:

$$\rho_{FIRB} = \frac{1}{10\pi} \rho_{MBR} \approx 0.032 \rho_{MBR} \quad 3.5.31$$

The ratio between FIRB and MBR corresponds to the value of 3.4% calculated by E. L. Wright [25].

In this Section we proposed a new component of the Medium of the World – BEC drops of dineutrinos whose mass about equals to Planck mass, and temperature of around 29 K. BEC drops are responsible for the FIRB and explain the substantial 100 micron flux in excess of expected zodiacal and Galactic emission.

The BEC drops do not absorb and re-emit starlight. Instead, they absorb energy directly from the Medium of the World. We can thus explain the existence of ultra-luminous infrared galaxies in a very active star formation period, which are extremely bright in the infrared spectrum and at the same time faint (often almost invisible) in the optical.

3.6. MULTI-COMPONENT DARK MATTER

The mystery about α is actually a double mystery. The first mystery - the origin of its numerical value $\approx 1/137$ has been recognized and discussed for decades. The second mystery – the range of its domain – is generally unrecognized.

Malcolm H. Mac Gregor

There are three prominent hypotheses on nonbaryonic DM, namely Hot Dark Matter (HDM), Warm Dark Matter (WDM), and Cold Dark Matter (CDM). In our Model, DM particle masses are proportional to m_0 multiplied by different exponents of α . Consequently, we can predict the masses of various types of DM particles:

CDM particles (fermions Neutralinos and WIMPs):

$$m_N = \alpha^{-2} m_0 = 1.3149950 \text{ TeV}/c^2 \quad 3.6.1$$

$$m_{WIMP} = \alpha^{-1} m_0 = 9.5959823 \text{ GeV}/c^2 \quad 3.6.2$$

DIRACs (bosons):

$$m_{DIRAC} = 2\alpha^0 \frac{m_0}{2} = 70.025267 \text{ MeV}/c^2 \quad 3.6.3$$

ELOPs (bosons):

$$m_{ELOP} = 2\alpha^1 \frac{m_0}{3} = 340.66606 \text{ keV}/c^2 \quad 3.6.4$$

WDM particles (sterile neutrinos have both Dirac and Majorana terms [6]):

$$m_{\nu_s} = \alpha^2 m_0 = 3.7289402 \text{ keV}/c^2 \quad 3.6.5$$

These values fall into the ranges estimated in literature (see [3] and references therein). In all, there are 5 different types of DM particles. Then the total energy density of DM is (see equation 3.5.18):

$$\rho_{DM} = 5\rho_p = 0.24007327\rho_{cr} \quad 3.6.6$$

Note that one of outstanding puzzles in particle physics and cosmology relates to so-called cosmic coincidence: the ratio of dark matter density in the World to baryonic matter density in the Medium of the World $\cong 5$ [60, 61].

The signatures of DM particles annihilation with predicted masses of 1.3 TeV, 9.6 GeV, 70 MeV, 340 keV, and 3.7 keV are found in spectra of the diffuse gamma-ray background and the emission of various macroobjects in the World (see Section 3.8).

3.7. MACROOBJECTS CORES BUILT UP FROM FERMIONIC DARK MATTER

In our opinion, all Macroobjects (MO) of the World (including galaxy clusters, galaxies, globular clusters, extrasolar systems, and planets) possess the following properties:

- Macroobject cores are made up of DM particles;
- Macroobjects consist of all particles under consideration, in the same proportion as they exist in the World's Medium;
- Macroobjects contain other particles, including DM and baryonic matter, in shells surrounding the cores.

The first phase of stellar evolution in the history of the World may be Dark Stars (DS), powered by Dark Matter heating rather than fusion. Neutralinos and WIMPs, can annihilate and provide an important heat source for the stars and planets in the World.

A Dark Star made up of heavier particles – WIMPs and neutralinos – could in principle have a much higher density. In order for such a star to remain stable and not exceed the nuclear density, WIMPs and neutralinos must partake in an annihilation interaction. According to WUM the maximum density of neutron stars equals to the nuclear density

$$\rho_{max} = \left(\frac{m_p}{m_0}\right)^4 \rho_0 = \beta^4 \rho_0 \quad 3.7.1$$

which is the maximum possible density of any macroobject in the World and $\beta = \frac{m_p}{m_0}$.

Table 1 and 2 summarize the parameter values for DS made up of various fermions:

Table 1

Fermion	Fermion relative mass m_f/m_0	Macroobject relative mass M_{max}/M_0	Macroobject relative radius R_{min}/L_g	Macroobject relative density ρ_{max}/ρ_0
Tauonic neutrino	$6 \times Q^{-1/4}$	$6^{-2} \times Q^{1/2}$	$6^{-2} \times Q^{1/2}$	$6^4 \times Q^{-1}$
Sterile neutrino	α^2	α^{-4}	α^{-4}	α^8
Preon	$3^{-1}\alpha^1$	$3^2\alpha^{-2}$	$3^2\alpha^{-2}$	$3^{-4}\alpha^4$
Electron-proton (white dwarf)	α^1, β	β^{-2}	$(\alpha\beta)^{-1}$	$\alpha^3\beta$
Monopole	2^{-1}	2^2	2^2	2^{-4}
WIMP	α^{-1}	α^2	α^2	α^{-4}
Neutralino	α^{-2}	α^4	α^4	α^{-8}
Interacting WIMPs	α^{-1}	β^{-2}	β^{-2}	β^4
Interacting neutralinos	α^{-2}	β^{-2}	β^{-2}	β^4
Neutron (star)	$\approx \beta$	β^{-2}	β^{-2}	β^4

where

$$M_0 = \frac{4\pi m_0}{3} \times Q^{3/2} \quad 3.7.2$$

$$L_g = a \times Q^{1/2} \quad 3.7.3$$

$$\rho_0 = \frac{hc}{a^4} \quad 3.7.4$$

Table 2

Fermion	Fermion mass $m_f, MeV/c^2$	Macroobject mass M_{max}, kg	Macroobject radius R_{min}, m	Macroobject density $\rho_{max}, kg/m^3$
Tauonic neutrino	4.50×10^{-8}	8.4×10^{50}	3.7×10^{24}	3.8×10^{-24}
Sterile neutrino	3.73×10^{-3}	1.2×10^{41}	5.4×10^{14}	1.8×10^{-4}
Preon	$\gtrsim 0.17$	5.9×10^{37}	2.6×10^{11}	7.8×10^2
Monopole	$\gtrsim 35$	1.4×10^{33}	6.2×10^6	1.4×10^{12}
Interacting WIMPs	9,596	1.9×10^{30}	8.6×10^3	7.2×10^{17}
Interacting neutralinos	1.315×10^3	1.9×10^{30}	8.6×10^3	7.2×10^{17}
Electron/proton (white dwarf)	0.511/938.3	1.9×10^{30}	1.6×10^7	1.2×10^8
Neutron (star)	939.6	1.9×10^{30}	8.6×10^3	7.2×10^{17}

Note that DS made up of strongly interacting neutralinos and WIMPs have the same mass and size as neutron star. The calculated parameters of DS show that

- White Dwarf Shells (WDS) around the nuclei made of strongly interacting WIMPs or neutralinos compose cores of stars in extrasolar systems;
- Shells of Dissociated DIRACs to Monopoles around the nuclei made of strongly interacting WIMPs or neutralinos form cores of globular clusters;
- Shells of Dissociated ELOPs to Preons around the nuclei made of strongly interacting WIMPs or neutralinos constitute cores of galaxies;
- Shells of Sterile neutrinos around the nuclei made of strongly interacting WIMPs or neutralinos make up cores of galaxy clusters;
- Shells of Tauonic neutrinos around the nuclei made of strongly interacting WIMPs or neutralinos reside in the cores of galaxy superclusters.

Although there are no free Dirac's monopoles and preons in the World, they can arise in the cores of Fermionic Compact Stars (FCS) as the result of DIRACs and ELOPs gravitational collapse with density increasing up to the nuclear density ($\sim 10^{17} \frac{kg}{m^3}$) and/or at high temperatures, with subsequent dissociation of dipoles to monopoles and preons.

The existence of supermassive objects in galactic centers is now commonly accepted. It is commonly believed that the central mass is a supermassive black hole. There exists, however, evidence to the contrary. In late 2013, ICRAR astronomer Dr. Natasha Hurley-Walker spotted a previously unknown radio galaxy NGC1534 that is quite close to Earth at 248 million light years, but is much fainter than it should be if the central black hole was accelerating the electrons in the jets: "*The discovery is also intriguing because at some point in its history the central black hole switched off but the radio jets have persisted. This is a very rare occurrence—this is only the fifth of this type to be discovered, and by far the faintest. We can only see it at low frequencies, which tells us that the electrons in the jets are not getting new energy from the black hole, so it must have been switched off for some time*" [62]. It's also possible there was never a black hole there at all.

Alternative models for the supermassive dark objects in galactic centers, formed by self-gravitating non-baryonic matter composed of fermions and bosons, are widely discussed in literature. According to WUM, the heaviest macroobjects include high-density preon plasma and sterile neutrinos shells around their cores:

- Macroobjects with a cold preon shell emit strong radio waves. Such objects are good candidates for the compact astronomical radio sources at centers of galaxies like Sagittarius A* in the Milky Way Galaxy [Wikipedia, Sagittarius A*].
- Red Giants are macroobjects with hot preon shells.
- Blazars are members of a larger group of active galaxies that host active galactic nuclei (AGN). They are macroobjects with hot preon and sterile neutrinos shells.
- Quasars are the most energetic and distant members of AGN. They are macroobjects with very hot preon and sterile neutrinos shells.

- Seyfert galaxies are one of the two largest groups of AGN, along with quasars. They have quasar-like nuclei, but unlike quasars, their host galaxies are clearly detectable. Seyfert galaxies account for about 10% of all galaxies [Wikipedia, Seyfert galaxy].

Note that the temperature of preon and sterile neutrinos shells depends on the composition of the macroobject core. Macroobjects whose cores are made up of WIMPs and preons remain cold. Macroobjects with cores made up of WIMPs and WDS produce hot preon and sterile neutrino shells. MO whose cores consist of neutralinos and WDS have very hot preon and sterile neutrino shells.

The mass of an AGN is about 7-11 orders of magnitude larger than the mass of the Sun. The radius of an AGN is about 4-7 orders of magnitude larger than the radius of WDS (see Table 2). The area of the closed spherical surface around the AGN is 8-14 orders of magnitude greater than the surface area of WDS. Luminosity of the AGN is then 8-14 orders of magnitude higher than the luminosity of the Sun. This take on an AGN explains the fact that *the most luminous quasars radiate at a rate that can exceed the output of average galaxies, equivalent to two trillion (2×10^{12}) suns* [Wikipedia, Quasar].

To summarize, macroobjects of the World have cores made up of DM particles. The cores are surrounded by shells made up of DM and baryonic matter. Every macroobject consists of all particles under consideration that are present in the same proportion as they exist in the World's Medium. No compact stars are made up solely of DM fermionic particles, for instance.

3.8. DARK MATTER SIGNATURES IN GAMMA-RAY SPECTRA

Large number of papers has been published in the field of X-ray and gamma-ray astronomy. The X-ray and gamma-ray background from $\lesssim 0.1 \text{ keV}$ to $\gtrsim 10 \text{ TeV}$ has been studied using high spectral and spatial resolution data from different spectrometers. Numerous papers were dedicated to Dark Matter searches with astroparticle data (see reviews [63-72] and references therein).

Dark Matter annihilation is proportional to the square of the DM density and is especially efficient in places of highest concentration of dark matter, such as compact stars built up from fermionic dark matter particles (see Section 3.7).

Recall that no macroobjects are made up of just a single type of DM particles, since other DM particles as well as baryonic matter are present in the shells. It follows that macroobjects cannot irradiate gamma rays in a single spectral range. On the contrary, they irradiate gamma-quants in different spectral ranges with ratios of fluxes depending on structure of a given macroobject.

The models of DM annihilation and decay for various types of macroobjects (galaxy clusters, blazars, quasars, Seyfert galaxies) are well-developed. Physicists working in the field X-ray and gamma-ray astronomy attempt to determine masses of DM particles that would fit the experimental results with the developed models.

WUM predicts existence of DM particles with 1.3 TeV, 9.6 GeV, 70 MeV, 340 keV, and 3.7 keV masses. We will look for signs of annihilation of these particles in the observed gamma-ray spectra. We connect gamma-ray spectra with the structure of macroobjects (core and shells composition).

3.8.1. NEUTRALINO 1.3 TEV

J. Holder has this to say about TeV Gamma-ray Astronomy: “*The mechanisms which drive the high energy emission from blazars remain poorly understood, and a full discussion is beyond the scope of this review. Briefly; in leptonic scenarios, a population of electrons is accelerated to TeV energies, typically through Fermi acceleration by shocks in the AGN jet. These electrons then cool by radiating X-ray synchrotron photons. TeV emission results from inverse Compton interactions of the electrons with either their self-generated synchrotron photons, or an external photon field. The strong correlation between X-ray and TeV emission which is often observed provides evidence for a common origin such as this, although counter examples do exist*” [73].

R.C.G. Chaves, et al. have this to say about Extending the H.E.S.S. Galactic Plane Survey: “*Approximately 100 VHE γ -ray sources have now (2009) been discovered [75-79]. Over two-thirds of these sources are located in our Galaxy. VHE γ -rays carry information about the most extreme environments in the local Universe, and although a significant fraction of the Galactic VHE (Very High Energy) γ -ray sources do not appear to have obvious counterparts at other wavelengths, the majority of them are associated with the violent, late phases of stellar evolution, e.g. supernova remnants (SNRs), pulsar wind nebulae (PWNe) of high spin-down luminosity pulsars, and massive Wolf-Rayet (WR) stars in stellar clusters*” [74].

O. Tibolla, et al. have this to say about New Unidentified H.E.S.S. Galactic Sources: “*Some of the unidentified H.E.S.S. sources have several positional counterparts and hence several different possible scenarios for the origin of the VHE gamma-ray emission; their identification remains unclear. Others have so far no counterparts at any other wavelength. Particularly, the lack of an X-ray counterpart puts serious constraints on emission models*” [75].

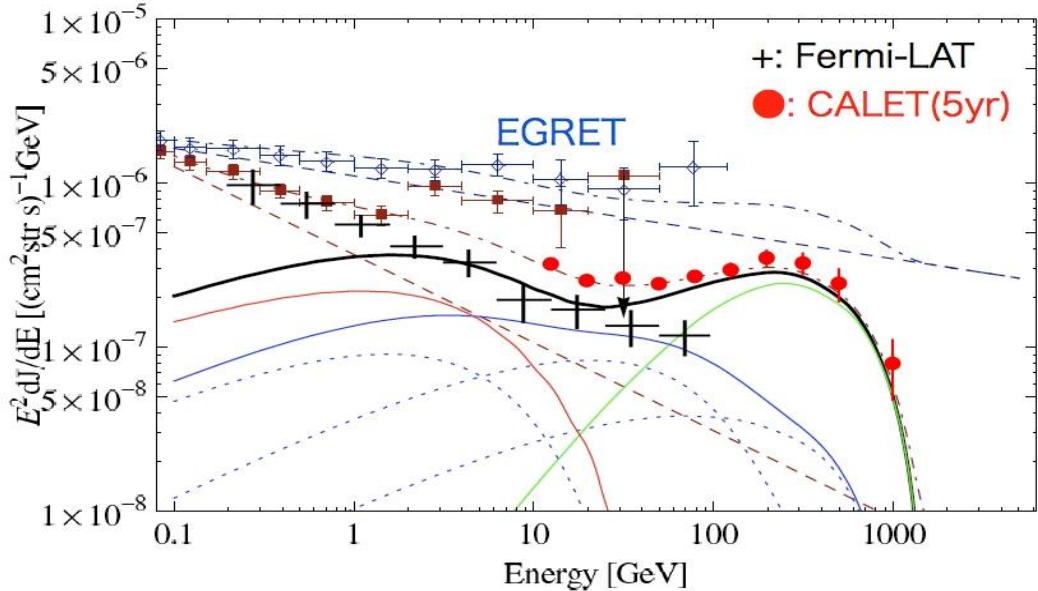
In our opinion, this correlation between keV emission and TeV emission can be easily explained by the annihilation of the sterile neutrinos (3.7 keV) in the shell around the core of AGN made of neutralinos (1.3 TeV). Moreover, the TeV blazar emission should be classified as extremely-hard X rays and not gamma rays, since by definition, *X rays are emitted by electrons outside the nucleus, while gamma rays are emitted by the nucleus*.

A detailed global analysis on the interpretation of the latest data of PAMELA, Fermi-LAT, AMS-02, H.E.S.S., and other collaborations in terms of dark matter annihilation and decay in various propagation models showed that for the Fermi-LAT and H.E.S.S. data favor $m_\chi \approx 1.3 \text{ TeV}$ [80-83]. This value of DM particle mass equals to the neutralino mass in our Model. The mass of the annihilating DM serves as the cutoff scale of the e^\pm spectrum. The lepton spectra must have a cutoff energy at the DM particle mass m_χ .

The obtained data in [84-92] require DM mass to be around 1 to 1.5 TeV which is in good agreement with the predicted mass of a neutralino. A. A. Abdo, et al. have this to say about Cosmic Ray $e^+ + e^-$ spectrum: “*The obtained spectra can be nicely fit by adding an additional component of primary electrons and positrons, with injection spectra $J(E) \propto E^{-\gamma} \exp\{-E/E_{cut}\}$ with the spectral index γ of about 3 and E_{cut} being the cutoff energy of the source spectra. Such an additional*

component also provides a natural explanation of the steepening of the spectra above 1 TeV indicated by the obtained data. Pulsars are the most natural candidates for such sources” [78].

In our opinion, results obtained by the CALET program are the closest to the ultimate discovery of the first confirmed dark matter particle - neutralino. Diffuse gamma-ray results anticipated for CALET in five years of investigations compared to the previous data and to model predictions are depicted in Figure 1. The anticipated results are in a very good agreement with the predicted mass of neutralino.



The presence of spectral break at 1.3 TeV in VHE spectra was measured for different blazars [128 - 132]. Some nearby sources, e.g. Vela, Cygnus Loop and Monogem Supernova Remnant (SNR) have unique signatures in the electron energy spectrum in the TeV region: broken power-law at $\sim 1.3 \text{ TeV}$ [133]. The DM interpretations of the $e \pm$ excesses observed by PAMELA, Fermi and ATIC give the mass of dark matter particles 1.3 TeV [134].

As we mentioned above, pulsars are the most natural candidates for such VHE gamma-ray sources. Wikipedia defines pulsar as a *highly magnetized, rotating neutron star that emits a beam of electromagnetic radiation. Neutron stars are very dense, and have short, regular rotational periods* [Wikipedia, Pulsar]. According to WUM, FCS made up of strongly interacting neutralinos and WIMPs have maximum mass and minimum size which are exactly equal to parameters of neutron stars (see Table 1 and 2). It follows that pulsars might be in fact rotating Neutralino stars and WIMP stars with different shells around them.

The cores of such pulsars may also be made up of the mixture of neutralinos (1.3 TeV) and WIMPs (9.6 GeV) surrounded by shells composed of the other DM particles: DIRACs (70 MeV), ELOPs (340 keV), and sterile neutrinos (3.7 keV). Annihilation of those DM particles can give rise to any combination of gamma-ray lines. Thus the diversity of VHE gamma-ray sources in the World has a clear explanation in frames of the World – Universe Model.

3.8.2. WIMP 9.6 GEV

In his review “Empirical Case for 10 GeV Dark Matter,” Dan Hooper summarized and discussed the body of evidence which has accumulated in favor of dark matter in the form of approximately 10 GeV particles, including *“the spectrum and angular distribution of gamma rays from the Galactic Center, the synchrotron emission from the Milky Way’s radio filaments, the diffuse synchrotron emission from the Inner Galaxy (the “WMAP Haze”) and low-energy signals from the direct detection experiments DAMA/LIBRA, CoGeNT and CRESST-II.* Dan Hooper finds that *“gamma-ray signal observed from the Galactic Center is consistent with 7-12 GeV dark matter particles annihilating mostly to leptons”* [93]. Dan Hooper and Lisa Goodenough estimated Dark Matter Annihilation in the Galactic Center and found that it fits into 7-10 GeV range [94].

In “EGRET Observations of the Extragalactic Gamma Ray Emission”, P. Sreekumar, *et al.* provide a graph of the all-sky observations in high-energy gamma rays from 30 MeV to 100 GeV (see Fig. 2). EGRET data on diffuse gamma-ray background show visible peaks around 70 MeV and 10 GeV. 10 GeV peak is consistent with annihilation of WIMPs. 70 MeV peak corresponds to annihilation of DIRACs (see Section 3.8.3).

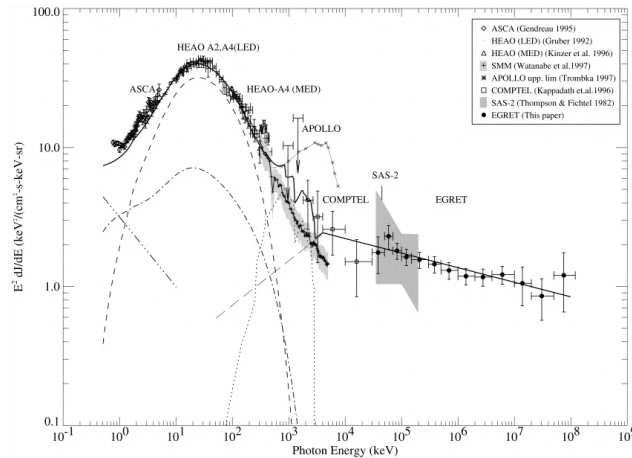


Figure 2. Multiwavelength spectrum of the extragalactic gamma rays; spectrum from X rays to high-energy gamma rays. The estimated contribution from Seyfert 1 (dot-dashed), and Seyfert 2 (dashed) are from the model of Zdziarski (1996); steep-spectrum quasar contribution (dot-dot-dashed) is taken from the paper of Chen et al. (1996); Type Ia supernovae (dot) is from the paper of Leising and Clayton (1993). The blazar contribution below 4 MeV (thin long dashed) is derived assuming the average blazar spectrum breaks around 4 MeV (McNaron-Brown, *et al.* 1995) to a power law with an index of ~ -1.7 . The thick solid line indicates the sum of all the components. Figure adapted from [95].

Based on EGRET observations, P. Sreekumar, *et al.* attribute the high-energy gamma ray emissions to blazars. *“Most of the measured spectra of individual blazars only extend to several GeV and none extend above 10 GeV, simply because the intensity is too weak to have a significant number of photons to measure”* [95]. WUM proposes that cores of blazars are composed of annihilating WIMPs (9.6 GeV), explaining why no observed radiation extends above 10 GeV.

The results of gamma-ray emission between 100 MeV to 10 GeV detected from 18 globular clusters in our Galaxy are also in a good correlation with the predicted mass of WIMPs. The gamma-ray spectra are generally described by a power law with a cut-off at a few GeV (1.4 – 7.1 GeV) [96, 97].

The DAMA/LIBRA, CoGeNT, CRESST-II, CDMS-II collaborations conduct direct detections of DM particles by nuclear recoils due to the elastic scattering of DM particles. The closest result to the predicted mass of WIMPs was obtained by CDMS-II collaboration which has reported 3 events in Si detector that are consistent with being nuclear recoils due to scattering of Galactic dark matter particles. An 8.6 GeV DM particle is deemed most probable [98].

Based on its core assumptions, WUM analytically predicts WIMPs to possess the mass of 9.6 GeV. A large number of experimental results seem to converge to a number in the neighborhood of 10 GeV, providing additional support to WUM.

3.8.3. DIRAC 70 MEV

C. Boehm, P. Fayet, and J. Silk propose a way “*to reconcile the low and high energy signatures in gamma-ray spectra, even if both of them turn out to be due to Dark Matter annihilations. One would be a heavy fermion for example, like the lightest neutralino (> 100 GeV [100]), and the other one a possibly light spin-0 particle (~ 100 MeV [100]). Both of them would be neutral and also stable as a result of two discrete symmetries (say R and M-parities)*” [99].

According to WUM, the two coannihilating DM particles are

- Neutralino (1.3 TeV) – a heavy fermion, and
- DIRAC (70 MeV) – a light spin-0 boson.

In Section 3.8.1 we discussed the observations of gamma rays in the very high-energy (> 100 GeV) domain [80-92] which are consistent with self-annihilating neutralino. In Section 3.8.2 we showed multiwavelength spectrum of the extragalactic gamma rays (Fig. 2) and mentioned the 70MeV peak.

S. D. Hunter, et al. discuss a “pion bump” centered at 67.5 MeV: “*Below about 100 MeV, gamma rays produced via electron bremsstrahlung are the dominant component of the observed spectrum, whereas, above about 100 MeV, the gamma-rays from π^0 decay, which form the broad “pion bump” centered at 67.5 MeV, are the dominant component of the spectrum. The “pion bump”, clearly visible in this spectrum, is the only spectral feature in the diffuse gamma ray emission in the EGRET energy range*” [101]. 70 MeV peak in EGRET data was discussed by Golubkov and Khlopov [102]. They explained this peak by the decay of π^0 -mesons, produced in nuclear reactions. B. Wolfe, et al. said that gamma rays at 70 MeV are notably detectable by GLAST and EGRET [103].

Another example of 70 MeV peak in the emission spectrum from an old supernova remnant (SNR) is shown in Figure 3. R. Yamazaki, et al. attribute the peak to π^0 -decay: “*When the SNR age is around 10^5 yrs., proton acceleration is efficient enough to emit TeV γ -rays both at the shock of the SNR and that in the giant molecular cloud (GMC). The maximum energy of primarily accelerated electrons is so small that TeV γ -rays and X-rays are dominated by Hadronic processes, π^0 -decay and synchrotron radiation from secondary electrons, respectively*” [104, 105].

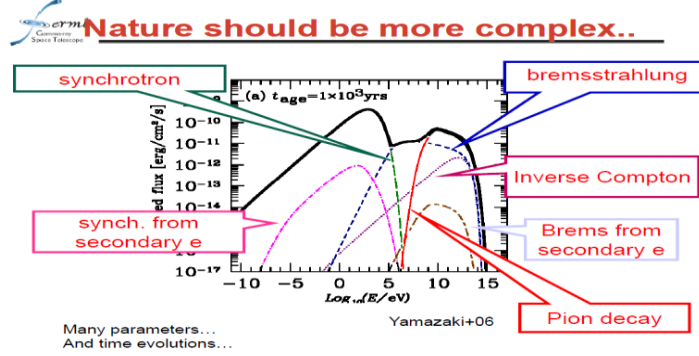


Figure 3. Spectrum of a single supernova remnant (SNR) with an age 1×10^3 years that stores energy, 10^{50} ergs, of high-energy protons. Figure adapted from [105].

Note that whenever the 70 MeV peak appears in gamma-ray spectra, it is always attributed to pion decay. We claim that π^0 decay produces a 67.5 MeV peak, while DIRAC annihilation is responsible for 70 MeV peak. Observation of the two distinct peaks is complicated by the broadness of the observed “pion bump”. We suggest utilization of exponentially cutoff power-law for analysis of experimental data for gamma-ray energies < 70 MeV. A better fit of experimental data will be evidence of DIRAC annihilation. DIRAC is a spin-0 boson with 70 MeV mass.

In our opinion, the DIRAC may indeed be the so-called U boson, target of intense search by the scientific community [106-111]. Note that the mass of DIRAC proposed by WUM – $0.07 GeV/c^2$ – falls into the mass range of U boson: $M_U = 0.02 - 0.1 GeV/c^2$.

3.8.4. ELOP 340 KEV

An ELOP is a spin-0 boson with 340 keV mass. Existence of DM particles of similar masses has been discussed by Y. Rasera, et al.: “*The diffuse gamma-ray background depends on three main quantities. The first is the annihilation cross-section: we are going to explore two extreme cases: S-wave and P-wave. The second ingredient is the dark matter mass density profile: we are going to test peaked distributions (Moore, $c=15$) and shallow ones (NFW, $c=15$). The last unknown quantity is the dark matter particle mass m_χ . Both the NFW S-wave case and the Moore P-wave reproduce the total flux of the bulge 511 keV emission with reasonable Dark Matter particle mass of the order of $m_\chi \cong 100$ MeV and $m_\chi \cong 1$ MeV respectively. On the opposite, the NFW P-wave case would require masses ($m_\chi < 0.42$ MeV) so small that they are unable to produce 511 keV photons*” [112].

The theoretical NFW P-wave case with mass $m_\chi < 0.42$ MeV discussed above is in good agreement with the experimental 100-400 keV “bump” [113] and with annihilating ELOPs with mass 340 keV proposed in our Model. In our view, there are two coannihilating DM particles at play that explain these bumps:

- WIMP (9.6 GeV) – a heavy fermion, and
- ELOP (340 keV) – a light spin-0 boson.

The extragalactic background spectrum between 1 keV and 10 GeV is presented in Figure 4 that shows a visible “bump” around 4 keV (see Section 8.3.5) and in the 100 – 400 keV range.

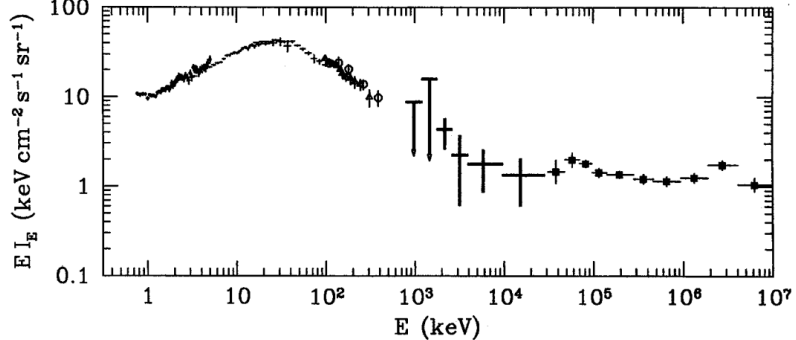


Figure 2. The high-energy extragalactic background spectrum from up-to-date measurements. The crosses marked by filled circles below 5 keV show the *ASCA* data as given by Gendreau (1995). The *ASCA* spectrum includes a Galactic contribution, significant below 1 keV. The spectral feature at ~ 2 keV is of instrumental origin. Crosses in the 3–100 keV range are from *HEAO-1* A2 and A4 LED measurements (Gruber 1992; see also Marshall et al. 1980; Rothschild et al. 1983). The data marked by open triangles and open circles are from *HEAO-1* A4 MED (Kinzer et al. 1996), and Nagoya balloon (Fukada et al. 1975) measurements, respectively. Note that both the *ASCA* and *HEAO-1* A4 MED data suggest that the normalization of the *HEAO-1* A2/A4 LED spectrum is somewhat underestimated. The bold crosses in the 0.8–30 MeV range are from COMPTEL (Kappadath et al. 1995), and the filled squares denote the data from EGRET (Sreekumar et al., in preparation).

Figure 4. Extragalactic background spectrum inspired by Figure 2 of A. A. Zdziarski [113].

D. E. Gruber, et al. describes a wide gamma-ray diapason as a sum of three power laws: “*Above 60 keV selected data sets included the HEAO 1 A-4 (LED and MED), balloon, COMPTEL, and EGRET data. The fit required the sum of three power laws, the flattest of which largely characterizes the EGRET observations (it ignores a likely “ripple” at 70 MeV), and the next steeper, with index 1.58, may be said to represent the spectrum between 70 keV and 1 MeV. The steepest component, with index 5.5, is almost certainly only a numerical necessity for matching to the lower energy spectrum and its derivative, and represents nothing physical*” [114].

According to our Model, the fit of the total diffuse spectrum in the range between 3 keV and 10 GeV should be performed based on three exponentially cutoff power-laws with injection spectral $J(E) \propto E^{-\gamma} \exp\{-E/E_{cut}\}$ with the spectral index γ and E_{cut} being the cutoff energy of the source spectra. For values of E_{cut} , we should use

- 9.6 GeV (annihilating WIMPs) in the 9.6 GeV – 70 MeV range;
- 70 MeV (annihilating DIRACs) in the 70 MeV – 340 keV range;
- 340 keV (annihilating ELOPs) in the 340 keV – 3.7 keV range.

The fit in the range between 9.6 GeV and 1.3 TeV should be done with $E_{cut} = 1.3$ TeV, which equals to the mass of a neutralino.

3.8.5. STERILE NEUTRINO 3.7 KEV

The Wikipedia overview of a sterile neutrino suggests the possibility of it being a Majorana fermion: *Unlike for the left-handed neutrino, a Majorana mass term can be added for a sterile neutrino without violating local symmetries (weak isospin and weak hypercharge) since it has no weak charge. However, this would still violate total lepton number. It is possible to include both Dirac and Majorana terms: this is done in the seesaw mechanism. In addition to satisfying the Majorana equation, if the neutrino were also its own antiparticle, then it would be the first Majorana fermion* [Wikipedia, Sterile neutrino].

The very first signature of the emission around 3.7 keV was found in 1967 by P. Gorenstein, R. Giacconi, and H. Gursky. In their “The Spectra of Several X-ray Sources in Cygnus and Scorpio” paper they analyzed the counting rate in the 2 – 5 keV range and found that “*the sources GX-10.7, +9.1, +13.5, and +16.7 are qualitatively different from Sco X-1, Cyg X-1 or Cyg X-2 in that the highest number of net counts is recorded in the bin centered at 3.75 keV*” [115].

An important result was obtained by S. Safi-Harb and H. Ogelman in 1997. In the “ROSAT and ASCA Observations of W50 Associated with the Peculiar Source SS 433” paper they reported that “*the observations of the X-ray lobes of the large Galactic source W50 [are] associated with the two-sided jets source SS 433. They noted that a continuum model (power law or thermal bremsstrahlung) plus a Gaussian improves the fit to region w2 slightly. However, a broken power-law model gives the best fit. The power-law indices are 1.9 and 3.6, with the break occurring at 3.7 keV. This result is also close to our findings for the spectral fitting of region e2 in the eastern lobe, except that the spectrum from the western lobe is softer*” [116].

T. Itoh analyzed the broad-band (3.0–50 keV) spectra of NGC 4388 in his PhD Thesis “Suzaku Studies of Time Variable X-ray Spectra of Edge-On Active Galactic Nuclei” (2007). He wrote: “*The ionized iron absorption line indicates the presence of an ionized reprocessing material in the line of sight, as well as the cold matter. At this point, there still remained line like residuals around 3.7 keV and 4.0 keV. We included two more Gaussians at these energies, to find that they are significant at similar levels as above*” [117].

A. M. Bykov, *et al.* confirm the 3.7 keV peak in their “Isolated X-ray – infrared sources in the region of interaction of the supernova remnant IC 443 with a molecular cloud”: “*The nature of the extended hard X-ray source XMMU J061804.3+222732 and its surroundings is investigated using XMM-Newton, Chandra, and Spitzer observations. The X-ray emission consists of a number of bright clumps embedded in an extended structured non-thermal X-ray nebula larger than 30" in size. Some clumps show evidence for line emission at ~ 1.9 keV and ~ 3.7 keV at the 99% confidence level. A feature at 3.7 keV was found in the X-ray spectrum of Src 3 at the 99% confidence level*” [118].

R. Fukuoka, *et al.* observed the peak as well: “*We found two line-like residuals at ~ 3.7 keV and ~ 3.0 keV. We therefore added two narrow Gaussians for these lines, and then obtained a nice fit. The first line was surely detected with ~ 3σ significance*” [119]. In 2012, A. Moretti, *et al.* measured the diffuse gamma-ray emission at the deepest level and with the best accuracy available today [120]. An emission like around 3.7 keV is clearly visible in Figure 5:

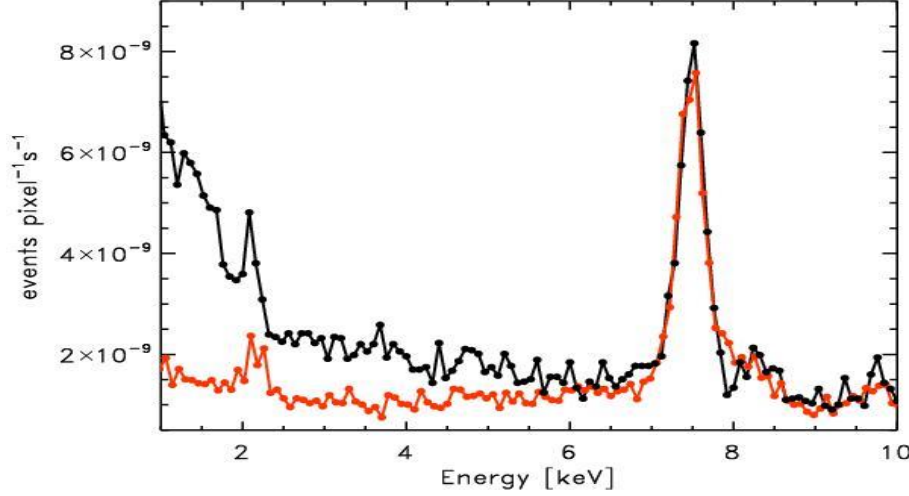


Figure 5. The energy channel (PI) distribution of the XPT unresolved emission (black) compared with the instrument background (red). In this plot PI channels have been transformed in energy using a single value and not the RMF matrix. The Figure adapted from [120].

3.8.6. CONCLUSION

- Emission lines of 1.3 TeV, 9.6 GeV, 70 MeV, 340 keV, and 3.7 keV, can be found in spectra of the diffuse gamma-ray background radiation and various macroobjects of the World in different combinations depending on their structure.
- The diffuse cosmic gamma-ray background radiation in the < 1.3 TeV range is the sum of the contributions of multicomponent self-interacting dark matter annihilation.
- The total cosmic-ray radiation consists of gamma-ray background radiation plus X-ray radiation from the different highly ionized chemical elements in the hot areas of the World and is due to various electron processes such as synchrotron radiation, electron bremsstrahlung, and inverse Compton scattering.

3.9. GRAND UNIFIED THEORY

At the very Beginning (Q=1) all extrapolated fundamental interactions of the World – strong, electromagnetic, weak, Super Weak and Extremely Weak (proposed in WUM), and gravitational – had the same cross-section of $\pi^2 a_0^2$, and were characterized by the Unified coupling constant:

$$\alpha_U = \alpha_S = \alpha_{EM} = \alpha_W = \alpha_{SW} = \alpha_{EW} = \alpha_G = 1 \quad 3.9.1$$

At that time, the extrapolated energy density of the World ρ_{cr0} was

$$\rho_{cr0} = 3 \frac{hc}{a^4} = 6.0638901 \times 10^{30} \frac{J}{m^3} \quad 3.9.2$$

which is four orders of magnitude smaller than the nuclear energy density ρ_{nuc} :

$$\rho_{nuc} = \left(\frac{m_p}{m_0}\right)^4 \frac{hc}{a^4} = 6.5151805 \times 10^{34} \frac{J}{m^3} \quad 3.9.3$$

The average energy density of the World has since been decreasing and its present value is given by

$$\rho_{cr} = \rho_{cro} \times Q^{-1} = 7.9775 \times 10^{-10} \frac{J}{m^3} \quad 3.9.4$$

The gravitational coupling parameter α_G is similarly decreasing:

$$\alpha_G = Q^{-1} \propto \tau^{-1} \quad 3.9.5$$

The weak coupling parameter is decreasing as follows:

$$\alpha_W = Q^{-1/4} \propto \tau^{-1/4} \quad 3.9.6$$

The strong and electromagnetic coupling parameters remain constant in time:

$$\alpha_S = \alpha_{EM} = 1 \quad 3.9.7$$

The difference in the strong and the electromagnetic interactions is not in the coupling parameters but in the strength of these interactions depending on the particles involved: electrons with charge e and monopoles with charge $\mu = \frac{e}{2\alpha}$ in electromagnetic and strong interactions respectively.

The super weak coupling parameter α_{SW} and the extremely weak coupling parameter α_{EW} proposed in our Model are decreasing as follows:

$$\alpha_{SW} = Q^{-1/2} \propto \tau^{-1/2} \quad 3.9.8$$

$$\alpha_{EW} = Q^{-3/4} \propto \tau^{-3/4} \quad 3.9.9$$

According to WUM, the super-weak interaction has coupling strength $\sim 10^{-10}$ times weaker than that of weak interaction. The possibility of such ratio of interactions was discussed in the developed theoretical models explaining CP and Strangeness violation [121-124]. Super-weak and Extremely-weak interactions provide an important clue to physics beyond the standard model.

The World – Universe Model is the first unified model of the World that successfully describes all of its primary parameters and their relationships, ranging in scale from cosmological structures to elementary particles. The Model allows for precise calculation of values that were only measured experimentally earlier (age of the World, MBR temperature, etc.), and makes verifiable predictions. While the Model needs significant further elaboration, it can already serve as a basis for a new Physics proposed by Paul Dirac in 1937.

Acknowledgements: I am very grateful to Felix Lev, my life-long friend, and my son Ilya Netchitailo for valuable stimulating discussions of 4-D Model.

References

1. P. A. M. Dirac, Nature, **139**, 323 (1937).
2. P. A. M. Dirac, Proc. R. Soc. Lond. **A**, **338**, 439 (1974).
3. V. S. Netchitailo, "World - Universe Model", <http://vixra.org/abs/1303.0077>.

4. V. S. Netchitailo, "Fundamental Parameter Q. Recommended Values of the Newtonian Parameter of Gravitation, Hubble's Parameter, Age of the World, and Temperature of the Microwave Background Radiation", <http://vixra.org/abs/1312.0179>.
5. V. S. Netchitailo, "World - Universe Model with Time Varying Gravitational Parameter", <http://vixra.org/abs/1401.0187>.
6. V. S. Netchitailo, "World - Universe Model. Fundamental parameters and Units", <http://vixra.org/abs/1402.0101>.
7. V. S. Netchitailo, "World - Universe Model. Multicomponent Dark Matter. Cosmic Gamma-Ray Background", <http://vixra.org/abs/1406.0018>.
8. V. S. Netchitailo, "World - Universe Model. Super-Weak Interaction. Sterile Neutrino Dark Matter", <http://vixra.org/abs/1406.0179>.
9. V. S. Netchitailo, "World - Universe Model. The Summary", <http://vixra.org/abs/1411.0079>.
10. V. S. Netchitailo, "World - Universe Model. Cosmic Far-Infrared Background", <http://vixra.org/abs/1412.0265>.
11. J. McCullagh, Transactions of the Royal Irish Academy, **21**, 17 (1839).
12. J. Swain (2010), arXiv: ge-qc/1006.5754.
13. H. Thirring, Physikalische Zeitschrift, **19**, 204 (1918).
14. Yu. Baryshev, Practical Cosmology, **2**, 60 (2008).
15. E. M. Burbidge, G. R. Burbidge, W. A. Fowler, F. Hoyle, Reviews of Modern Physics **29**, 547 (1957).
16. J. W. Alsop, Jr. www.tesla-coil-builder.com/Articles/july_11_1934b.htm
17. Y. Nambu, Prog. Theor. Phys., **7**, 131 (1952).
18. M. H. Mac Gregor. *The Power of Alpha*, World Scientific, Singapore (2007).
19. C. Csaki, N. Kaloper, and J. Terning (2001), arXiv: hep-ph/0112212.
20. B. Pontecorvo and Ya. Smorodinski, Sov. Phys. JETP, **14**, 173 (1962).
21. R. A. Battye, A. Moss (2014), arXiv: astro-ph.CO/1308.5870 v2.
22. M. G. Hauser *et al.*, ApJ, **278**, L15 (1984).
23. F. J. Low *et al.*, ApJ, **278**, L19 (1984).
24. B. Wang, ApJ, **374**, 465 (1991).
25. E. L. Wright, <http://www.astro.ucla.edu/~wright/CIBR/>.
26. D. J. Fixsen *et al.*, ApJ, **473**, 576 (1996).
27. D. P. Finkbeiner, M. Davis, and D. J. Schlegel (1999), arXiv: astro-ph/9905128.

28. B. T. Draine and A. Lazarian, *ApJ*, **508**, 157 (1998).
29. D. P. Finkbeiner and D. J. Schlegel (1999), arXiv: astro-ph/9907307.
30. G. Lagache et al. (1999), arXiv: astro-ph/9901059.
31. D. P. Finkbeiner, M. Davis, and D. J. Schlegel (2000), arXiv: astro-ph/0004175.
32. P. H. Siegel, *IEEE Transactions on Microwave Theory and Techniques*, **50**, No. 3, 910 (2002).
33. T. G. Phillips and J. Keene, *Proc. IEEE*, **80**, 1662 (1992).
34. X. Dupac *et al.* (2003), arXiv: astro-ph/0305230.
35. J. E. Aguirre et al. (2003), arXiv: astro-ph/0306425.
36. A. Pope et al. (2006), arXiv: astro-ph/0603409.
37. J. A. Marshall et al. (2007), arXiv: astro-ph/0707.2962.
38. M. J. Devlin et al. (2009), arXiv: astro-ph/0904.1201.
39. E. L. Chapin et al. (2010), arXiv: astro-ph/1003.2647.
40. T. Mackenzie et al. (2010), arXiv: astro-ph/1012.1655.
41. P. Serra et al. (2014), arXiv: astro-ph/1404.1933.
42. B. Hammel, <http://graham.main.nc.us/~bhammel/PHYS/planckmass.html>
43. W. Altmannshofer *et al.* (2009), arXiv: hep-ph/0902.0160 v2.
44. P. del Amo Sanchez *et al.* (2011), arXiv: hep-ex/1009.1529 v2.
45. S.-J. Sin (1992), arXiv: hep-ph/9205208 v1.
46. V. H. Robles and T. Matos (2012), arXiv: astro-ph/1201.3032 v1.
47. J. Magana *et al.* (2012), arXiv: astro-ph/1201.6107 v1.
48. A. Suarez, V. H. Robles, and T. Matos (2013), arXiv: astro-ph/1302.0903 v1.
49. A. Diez-Tejedor, A. X. Gonzalez-Morales, and S. Profumo (2014), arXiv: astro-ph/1404.1054 v2.
50. P. Sikivie and Q. Yang (2009), arXiv: hep-ph/0901.1106 v4.
51. O. Erken *et al.* (2011), arXiv: astro-ph/1111.3976 v1.
52. N. Banik and P. Sikivie (2013), arXiv: astro-ph/1307.3547 v1.
53. S. Davidson and M. Elmer (2013), arXiv: hep-ph/1307.8024 v2.
54. M.-H. Li and Z.-B. Li (2014), arXiv: astro-ph/1406.1312 v2.
55. M. Morikawa, 22nd Texas Symp. on Relativistic Astrophysics at Stanford University, 1122, 2004.

56. L. J. Garay *et al.* (2000), arXiv: gr-qc/0002015 v2.
57. M. Ueda and K. Huang (1998), arXiv: cond-mat/9807359 v1.
58. A. A. Hujeirat (2011), arXiv: gr-qc/1109.3821 v1.
59. F. Kuhnel and B. Sundborg (2014), arXiv: hep-th/1405.2083 v2.
60. W. Z. Feng, A. Mazumdar, P. Nath (2013), arXiv: 1302.0012 v2.
61. W. Z. Feng, P. Nath, G. Peim (2012), arXiv: 1204.5752 v2.
62. D. Cahill, Radio galaxy discovery near Earth spurs more questions (May 23, 2014).
<http://www.sciencewa.net.au/topics/space/item/2837-radio-galaxy-discovery-near-earth-spurs-more-questions>
63. L. E. Strigari (2012), arXiv: 1211.7090 v1.
64. K. Bechtol (2011) <http://astro.fnal.gov/events/Seminars/Slides/Bechtol%20120611.pdf>
65. J. H. Buckley, *et al.* (2008), arXiv: 0810.0444 v1.
66. T. Jeltema, 2011<http://www2011.mpe.mpg.de/erosita/erosita2011/program/PDF/jeltema.pdf>
67. F. A. Aharonian (2004) <http://www.worldscientific.com/worldscibooks/10.1142/4657>
68. T. Totani (2009) <http://www-conf.kek.jp/past/HEAP09/ppt/1day/Totani HEAP09.pdf>
69. R. P. Johnson, R. Mukherjee, New J. Phys. **11**, 055008 (2009).
70. F. Giovanneli, L. Sabau-Graziati, Mem. S. A. It. **83**, 17 (2012).
71. R. Essig, *et al.* (2013), arXiv: 1309.4091 v3.
72. T. A. Porter, R. P. Johnson, P. W. Graham (2011), arXiv: 1104.2836 v1.
73. J. Holder (2012), arXiv: 1204.1267 v1.
74. R. C. G. Chaves, *et al.* (2009), arXiv: 0907.0768 v1.
75. O. Tibolla, *et al.* (2009), arXiv: 0907.0574 v1.
76. S. Hoppe, *et al.* (2009), arXiv: 0906.5574 v2'
77. P. H. T. Tam, *et al.* (2009), arXiv: 0911.4332 v2.
78. O. Tibolla, *et al.* (2009), arXiv: 0912.3811 v1.
79. P. H. T. Tam, *et al.* (2010), arXiv: 1001.2950 v1.
80. J. Aleksic, *et al.* (2013), arXiv: 1312.1535 v3.
81. A. Moralejo (2013) <http://projects.ift.uam-csic.es/multidark/images/moralejoalcala.pdf>

82. A. Abramowski, *et al.* (2013), arXiv: 1301.1173 v1.
83. H. B. Jin, Y. L. Wu, Yu. F. Zhou (2013), arXiv: 0905.0025 v1.
84. A. A Abdo, *et al.* (2009), arXiv: 0905.0025 v1.
85. O. Adriani, *et al.* (2011), arXiv: 1103.2880 v1.
86. X. G. He (2009), arXiv: 0908.2908 v2.
87. I. Cholis, L. Goodenough (2010), arXiv: 1006.2089 v2.
88. A. Morselli, Progress in Particle and Nuclear Physics **66**, 208 (2011).
89. K. N. Abazajian, J. P. Harding (2011), arXiv: 1110.6151 v3.
90. N. Kawanaka, *et al.* (2010), arXiv: 1009.1142 v3.
91. F. A. Aharonian, *et al.*, Phys. Rev. Lett. **101**, 261104 (2008).
92. D. Granger <http://calet.phys.lsu.edu/Science/DGR.php>
93. D. Hooper (2012), arXiv: 1201.1303 v1.
94. D. Hooper, L. Goodenough (2010), arXiv: 1010.2752 v3.
95. P. Sreekumar, *et al.* (1997), arXiv: 9709257 v1.
96. A. A. Abdo, *et al.* (1997), arXiv: 1003.3588 v2.
97. P. H. T. Tam, *et al.* (1997), arXiv: 1207.7267 v1.
98. M. T. Frandsen, *et al.* (2013), arXiv: 1304.6066 v2.
99. C. Boehm, P. Fayet, J. Silk (2003), arXiv: 0311143 v1.
100. C. Boehm, *et al.* (2003), arXiv: 0309686 v3.
101. S. D. Hunter, *et al.*, The Astrophysical Journal, **481**, 205, E240 (1997).
102. Yu. A. Golubkov, M. Yu. Khlopov (2000), arXiv: 0005419 v1.
103. B. Wolfe, *et al.* (2008), arXiv: 0807.0794 v1.
104. R. Yamazaki, *et al.* (2006), arXiv: 0601704 v2.
105. T. Nakamori (2008) www.heap.phys.waseda.ac.jp/cnf1203/Files/Oral/Nakamori.pdf
106. G. Agakishiev, *et al.* (2013), arXiv: 1311.0216 v1.
107. H. Merkel, *et al.*, A1 Collaboration, Phys. Rev. Lett. **106**, 251802 (2011).
108. S. Abrahamyan, *et al.*, APEX Collaboration, Phys. Rev. Lett. **107**, 191804 (2011).
109. R. Meijer, *et al.*, SINDRUM I Collaboration, Phys. Rev. **D 45**, 1439 (1992).

110. P. Adlarson, *et al.*, WASA-at-COSY Collaboration, Phys. Lett. **B** **726**, 187 (2013).
111. D. Babuski, *et al.*, KLOE-2 Collaboration, Phys. Lett. **B** **720**, 111 (2013).
112. Y. Rasera, *et al.* (2006), arXiv: 0507707 v2.
113. A. A. Zdziarski, Mon. Not. R. Astron. Soc. **281**, L9 (1996).
114. D. E. Gruber, J. L. Matteson, and L. E. Peterson (1999), arXiv: 9903492 v1.
115. P. Gorenstein, R. Giacconi, and H. Gursky, The Astrophysical Journal, **150**, L85 (1967).
116. S. Safi-Harb, H. Ogelman, The Astrophysical Journal, **483**, 868 (1997).
117. T. Itoh, *Suzaku Studies of Time Variable X-ray Spectra of Edge-On Active Galactic Nuclei*, PhD Thesis (2007) http://www.astro.isas.jaxa.jp/suzaku/bibliography/phd/titoh_dron_print080220.pdf
118. A. M. Bykov, *et al.* (2009), arXiv: 0801.1255 v1.
119. R. Fukuoka, *et al.* (2008), arXiv: 0903.1906 v1.
120. A. Morretti, *et al.* (2012), arXiv: 1210.6377 v1.
121. L. Wolfenstein, Comments Nucl. Part. Phys., **21**, 275 (1994).
122. Y. Yamaguchi, Progress of Theoretical Physics, **22**, 373 (1959).
123. K. F. Kelley, Measurement of the CP Violation Parameter $\sin 2\beta$, PhD Thesis, MIT (1999).
124. B. A. Bian, *et al.* (2006) <http://ribll.impCAS.ac.cn/conf/ccast05/doc/RIB05-zhangfengshou.pdf>
125. Voyager. *The interstellar Mission*, June 14 (2012).
126. D. O. Gough, Solar Physics, **74**, 21 (1981).
127. C. LaRocco, B. Rothstein, The Big Bang, www.umich.edu/~gs265/bigbang.htm
128. M. Orr, F. Krennrich, E. Dwek (2011) ftp://cr0.izmiran.ru/Proceedings/%28ICRC%29/32th-ICRC_2011_Beijing/papers/OG2.3/icrc0960.pdf
129. M. Orr, F. Krennrich for the CTA Consortium (2011) http://www.ihep.ac.cn/english/conference/icrc2011/paper/proc/v8/v8_1156.pdf
130. M. Orr, F. Krennrich, E. Dwek (2011), arXiv: 1101.3498 v3.
131. A. Madhavan, *The VHE γ -ray spectra of several hard-spectrum blazars from long-term observations with the VERITAS telescope array*, PhD Thesis (2013).
132. http://iopscience.iop.org/0004-637X/733/2/77/fulltext/apj388425t1_ascii.txt
133. S. Torii for the CALET Collaboration (2014) http://www.crlab.wise.sci.waseda.ac.jp/eng/wp-content/uploads/downloads/2014/09/VHEPU2014-CALET_final.pdf
134. M. Papuccia and A. Strumia (2009), arXiv: 0912.0742 v1.